1949-08

An investigation of dynamic stresses in a landing gear at a pre-determined strut angle

Turner, Burr Van

St. Paul, Minnesota; University of Minnesota

http://hdl.handle.net/10945/6445

AN INVESTIGATION OF

DYNAMIC STRESSES IN A LANDING GEAR

AT

A PRE-DETERMINED STRUT ANGLE

A Thesis

Submitted to the Graduate Faculty

of the

University of Minnesota

by

Burr V.an Turner

In partial fulfillment of the requirements for

the Degree of

Master of Science in Aeronautical Engineering

August, 1949

PREFACE

During the history of aviation the stresses and strains which occur in landing gears during the initial part of landing an airplane have not been thoroughly investigated. In this thesis a study was made of the stresses and deflections which occurred upon landing. The response and forces resulting from these dynamic loads will be of primary concern.

The testing apparatus is located in building No. 717, Rosemount Research Center, Rosemount, Minnesota.

The reference material used in developing this theory, consisting of periodicals and engineering texts, were obtained from the aeronautical engineering office and the engineering library of the University of Minnesota.

The author is greatly indebted to Professor J. A. Wise for his guidance and valuable assistance in the preparation of this paper. Thanks is also due H. Wood for his liberal collaboration in the construction, design and testing activities.

B. V. T.

Minneapolis--August, 1949.

TABLE OF CONTENTS

TABLE OF FIGURES

SUMMARY

This is a preliminary study of the dynamic conditions of a landing gear and covers a range from light to above average landings. The weight assumed is approximately two-fifths of the normal static load on a landing gear. In actual landings an airplane wing still has lift during its initial phase, therefore, these assumptions are reasonable.

The experimental work covers the dropping range from two to five feet per second with varying tire pressures from twenty-four to forty pounds per square inch. These two parameters are the only conditions varied in this report.

A theoretical sample problem is worked for these conditions: A tire is assumed with 30 pounds per square inch pressure carrying a total weight of one thousand and sixty pounds and having a dropping velocity of four feet per second.

A comparison of this problem is made with the experimental values. The results indicate that the theoretical force is 22 per cent greater than the recorded data. The period resulting from setting up the equations of motion show that it is two and one half per cent less than that measured.

A moving picture was made of the dropping operations and is available to show the action in slow motion. It is filed in Visual Education, Westbrook Hall, University of Minnesota under Aeronautical Engineering Films.

INTRODUCTION

This thesis is the initial study in a projected series of reports concerning the stresses, strains, deflections and general information of a landing gear. This is part of a plan created by the Aeronautical Engineering Department, University of Minnesota. Only a limited phase of the subject will be covered in this paper since the scope of the field is far reaching. The reason for this limitation is that excessive time was required in the original construction of the testing apparatus.

First, a method had to be devised to simulate controlled landings similar to those encountered in an aircraft. This set-up was required to be in a laboratory so that accurate readings could be observed and recorded.

A Navy SNJ landing gear was used for testing purposes. The range of tire pressure was from 24 to 40 pounds per square inch, while the sinking speeds were varied from 2 to 5 feet per second. These ranges were chosen as being close to conventional landing conditions.

The present data gives sufficient information to verify the theory, but more recordings would have given a clearer picture.

APPARATUS AND INSTRUMENTS

The problem required a setup which would simulate the actual landing of an aircraft. A large flywheel was desired which would withstand heavy weights and could be revolved at speeds equivalent to those of landings. When a flywheel ten feet in diameter was found, an old reduction gear and test engine were used for power. This combination took care of turning such a large disc. With this material on hand the drawings of the pit and assembly were made.

The final assembly is shown in Fig. No. 1.

Fig. No. 1

The driving mechanism is illustrated in Fig. No. 2.

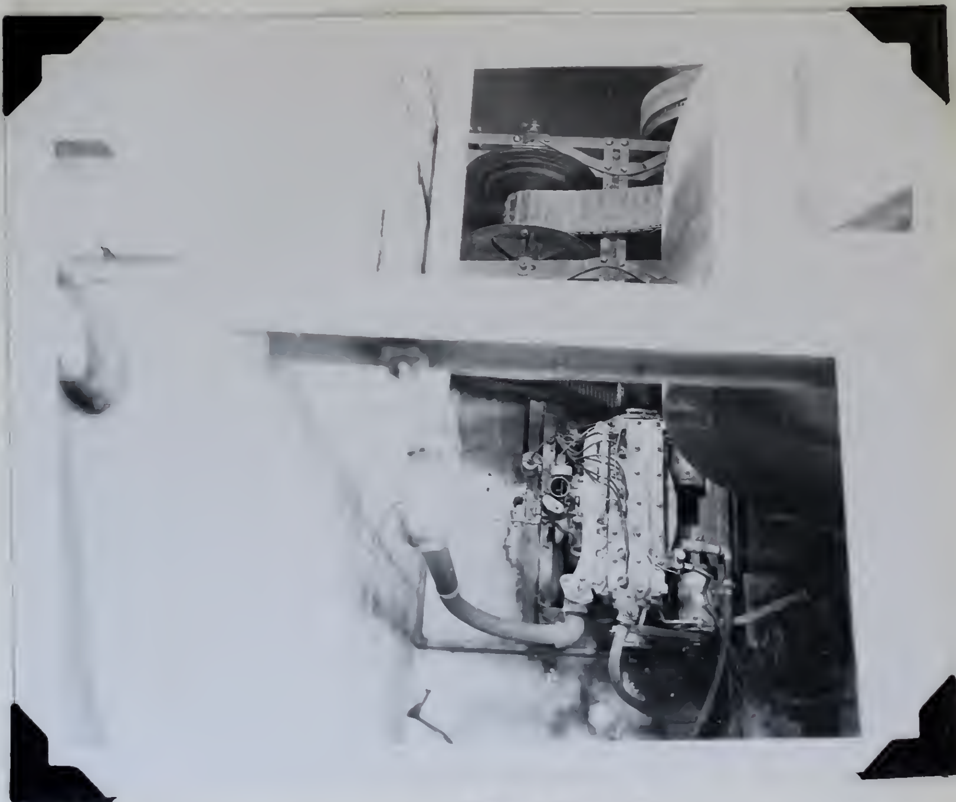

Fig. No. 2

After the apparatus was constructed type C-1, SR-4, strain gauges, made by Baldwin Southwark Division of the Baldwin Locomotive Works, were placed on the lower brace of the landing gear in a to and aft position opposite each other so the drag forces could be measured. Also, gauges were placed perpendicularly to those formerly mentioned in order to measure the axial forces. To determine the relative displacements between the oleo and the strut itself a potentiometer with a scissors lever arm was installed. A cantilever with damper was placed in an appropriate position, and strain gauges were properly located to measure the movement and deflec-

tion of the wheel. These gauges can be seen in Fig. No. 3.

Fig. No. 3

The leads from the strain gauges and the potentiometer were brought into a Brush Recorder which recorded the different forces and amplitudes. The weight of the gear was determined by using platform scales and a lever system - Fig. No. 4.

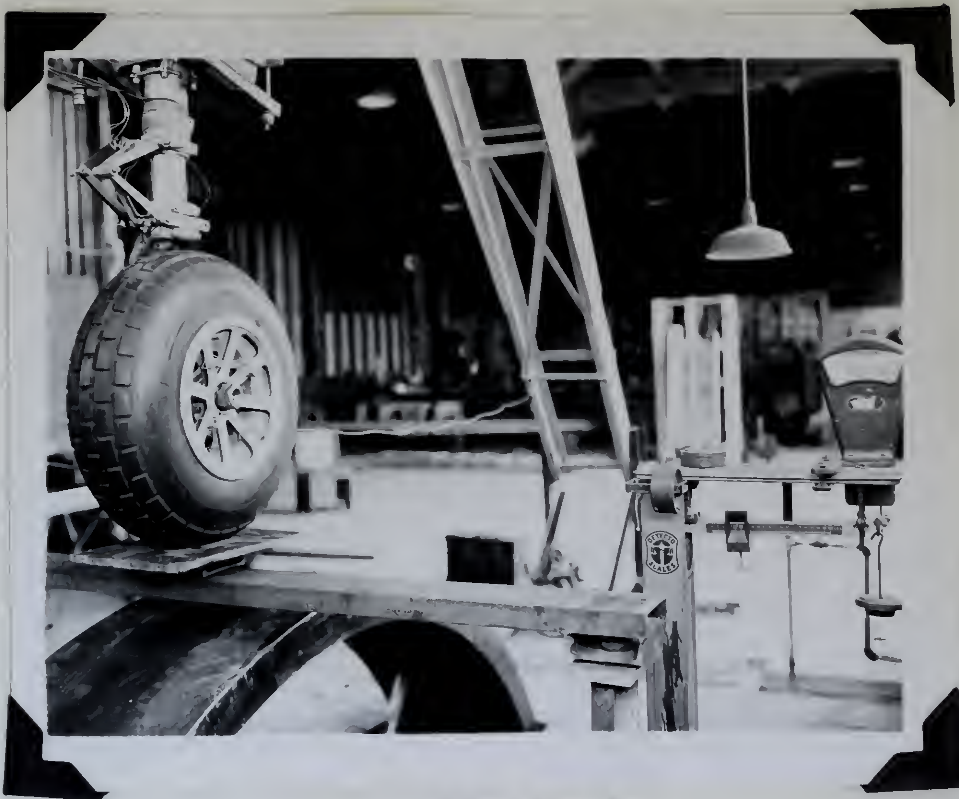

Fig. No. 4.

TESTING PROCEDURE

The method used in calibrating these three pairs of strain gauges and the one potentiometer are as follows:

(A) Axial Force. The two opposite gauges on the fork running parallel to the axis of the strut measure this force. The strain analyser was balanced and no load conditions were recorded. In this manner a relationship was established between the deflection of the oscilloscope and the vertical load applied. A full static load was applied and again readings were recorded. In other words, so many millimeters of deflection on the recorder indicated a known amount of force. Points between full load and no load were checked and found in agreement.

(B) Drag Force. These forces were obtained in a manner very similar to those mentioned above. Attention should be called to the procedure in which a horizontal pressure was applied to the strut. A light cable was stretched through a pulley where a known weight could be suspended. The cable can be seen in Fig. Nos. 1, 3, and 4. Here, with known loads, the recorder was calibrated.

(C) Cantilever Deflections. The displacement of the cantilever was measured by adjusting the landing gear a known distance above the flywheel; then by

lowering the gear a known deflection was incurred. This deflection was recorded on the Brush Recorder. A relation between landing wheel movement and the recording instrument was established through this action.

(D) Potentiometer. The potentiometer was the only article in the instrumentation which was not linear in recording characteristics. Here the oleo was deflected a prescribed amount and recordings were made. This was necessary because the potentiometer was operated by a scissors arrangement, and even under these conditions the values approached a straight line.

Testing procedure was begun when all the instruments were tested and calibrated. In order to operate the mechanism the Essex (test engine) was started and allowed to attain a fair rate of speed before engaging the reduction gear. Due to the weight of the large flywheel it was necessary to turn it over manually before tying in the drive system. Even under these conditions there was a great deal of slipping in the belting arrangement. This slipping occurred until the flywheel reached an approximate speed of twenty-five revolutions per minute. From this point the engine assumed control and was able to develop the speeds which were obtained during this study. The speeds were measured by a strobotac.

Upon reaching certain flywheel speeds, the operation shifted to where the strain gauges and controls for dropping had been placed. A quick release mechanism

was fastened to an overhead hoist and elevated the dropping arm to a height which would give the desired sinking speed. Drops were made from heights to represent one to seven feet per second velocity at striking.

When the dropping arm was at a desired level the apparatus was ready to simulate a landing. The Brush oscilloscopes were started and the quick release mechanism was tripped. The forces and deflections which occurred during the first few seconds of each landing were recorded. This procedure was repeated for the various dropping heights and tire pressures until the data was completed.

Motion pictures were made of drops, Fig. Nos. 10 through 12, at a rate of one hundred frames per second.

DISCUSSION

A strut angle of twenty-four degrees was chosen as the optimum angle of suspension. It was used as a point of departure for this thesis work and was suggested from another thesis developed simultaneously by H. Wood.[1] Only the forces up and down the strut are considered in developing the theory. This decision was made since the gear was in what was estimated to be the best angle.

The horizontal force problem which is neglected in this study is mentioned in the following remarks:

First: This force may be solved by equating internal energy to the external energy, but varying sectional moments of inertia pose another condition.

Second: In noting Fig. Nos. 8 to 23 inclusive, the drag and axial forces act in a uniform manner. Studying the areas under the force time curves might lead to a solution.

Third: A dynamic study of bearing friction and friction when striking contacts are made, may point to an answer of the drag force resulting from landing. Drag force is a function of friction and is of major

---

[1] "A Study of Dynamic Forces in Aircraft Landing Gear Struts with Relation to the Optimum Angle of Suspension", H. Wood, A Thesis for Degree of Master of Science in Aeronautical Engineering, July, 1949.

importance. A system of vectors and a knowledge of abrasion might suggest a solution.

The damping constant of the oleo was computed as follows for all the runs taken at twenty-four degrees. The axial force was known at a given time along with the spring constant of the strut. The amount by which the landing gear deflected for the above period of time was also known. These, too, were obtained from Fig. Nos. 8 through 23. Since

$$F = C\dot{X} + kX$$

C can be obtained. Following this the average value of C from all the readings was computed.

The spring constants for the system were computed by applying static loads to the gear and measuring the deflections of the tire and oleo. By repeating this process a sufficient number of times a rather constant graph was obtained, Fig. No. 7.

The original proposal of this thesis was to study the variations of five parameters, but because of mechanical failure of the driving apparatus only two--dropping velocity and tire pressure--were investigated.

In the design of the apparatus a curvilinear drop is used instead of a true vertical motion. A pivot point is located in line with the top of the large fly-wheel joining a dropping arm. Therefore, from the time the tire initially touches the landing surface and until

the strut is completely deflected, the landing strut changes angle from one to two degrees. The amount of change depends on the original angle setting. The suspension angle is the angle referred to when the scissors of the gear are closed.

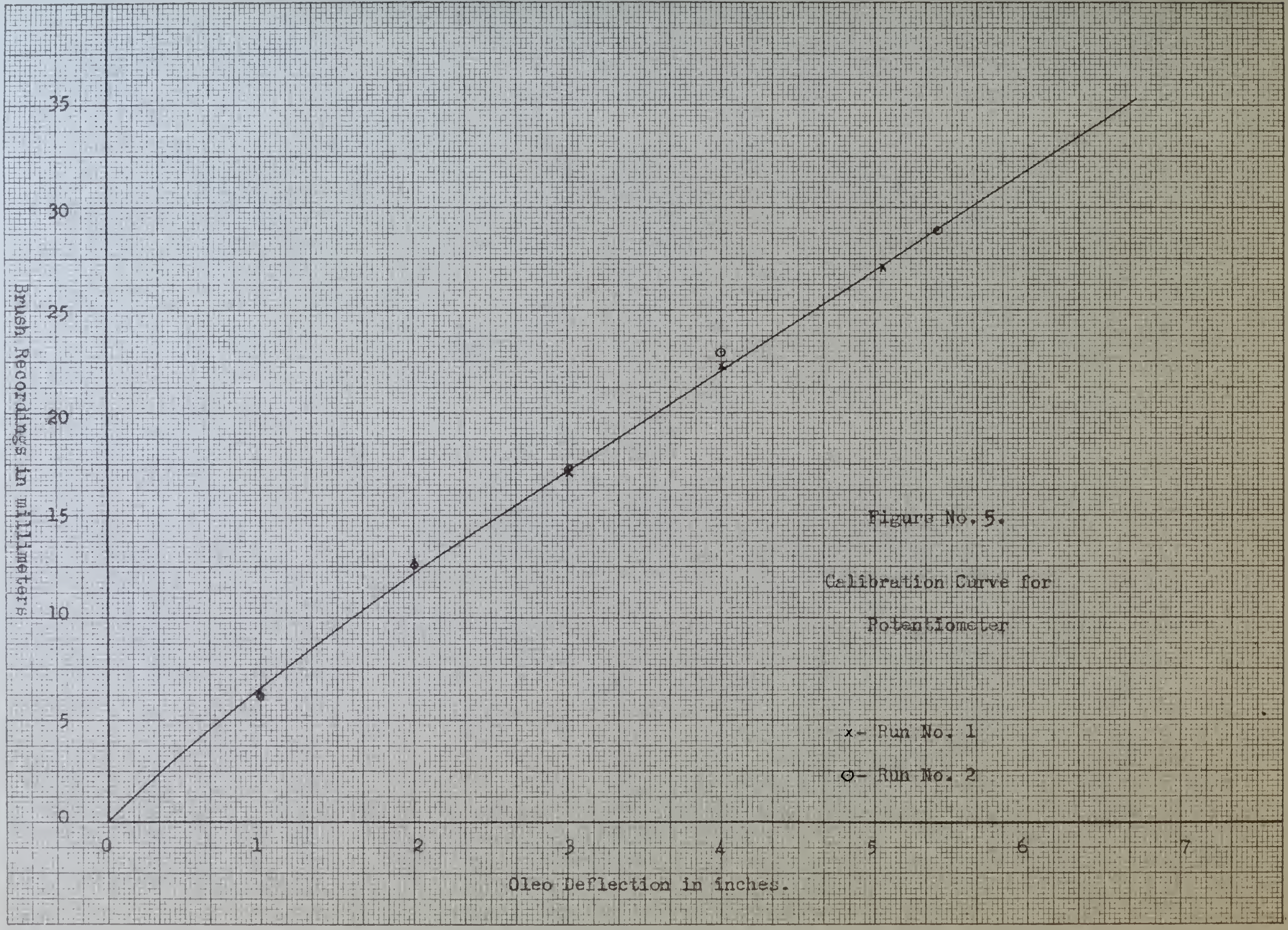
Figure No. 5.
Calibration Curve for
Potentiometer
x - Run No. 1
⊙ - Run No. 2
Brush Recordings in millimeters
35
30
25
20
15
10
5
0
0
1
2
3
4
5
6
7
Oleo Deflection in inches.

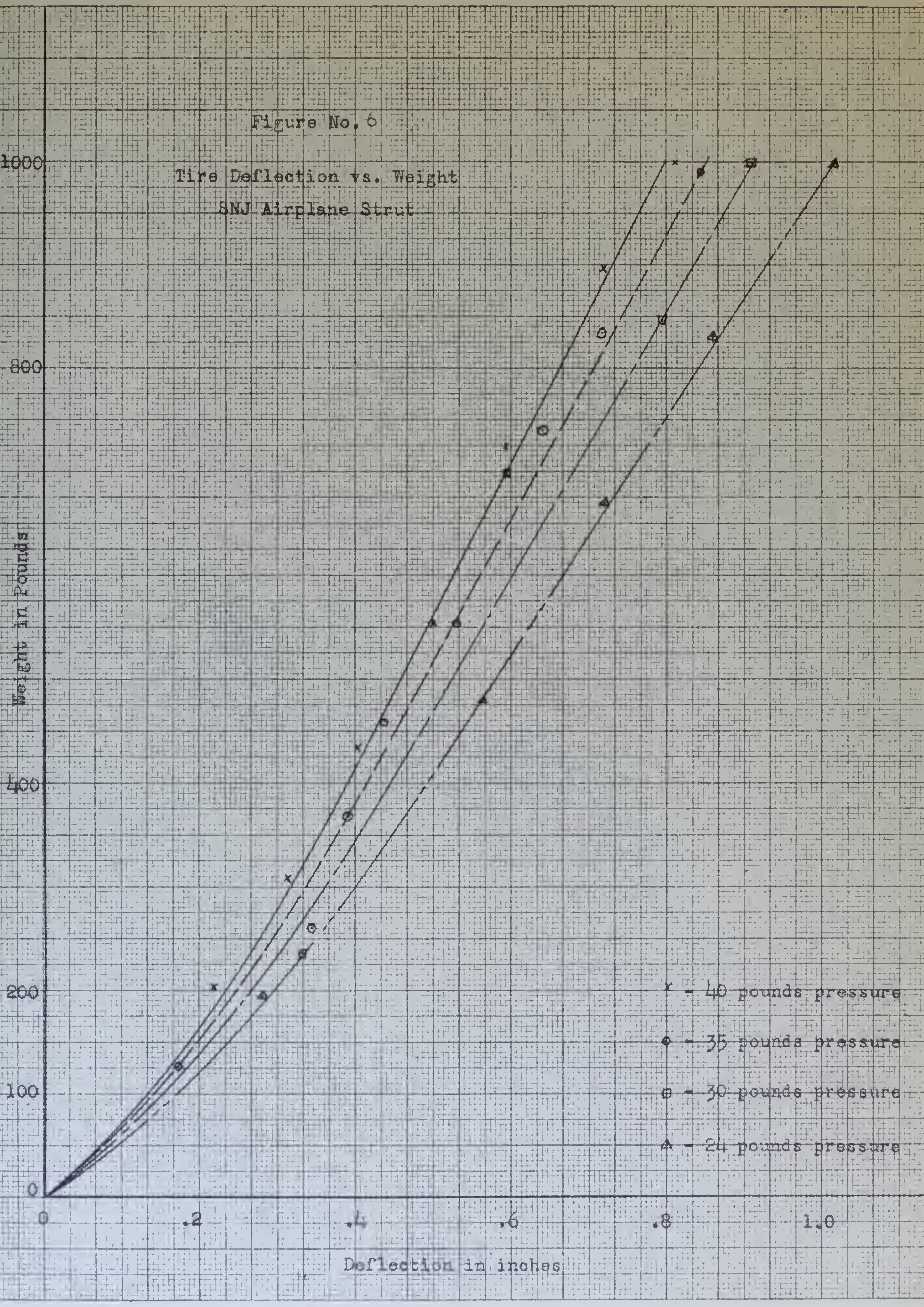

Figure No. 6
Tire Deflection vs. Weight
SNJ Airplane Strut
Weight in Pounds
Deflection in inches
1000
800
400
200
100
0
0
.2
.4
.6
.8
1.0
x - 40 pounds pressure
⊕ - 35 pounds pressure
⊡ - 30 pounds pressure
△ - 24 pounds pressure

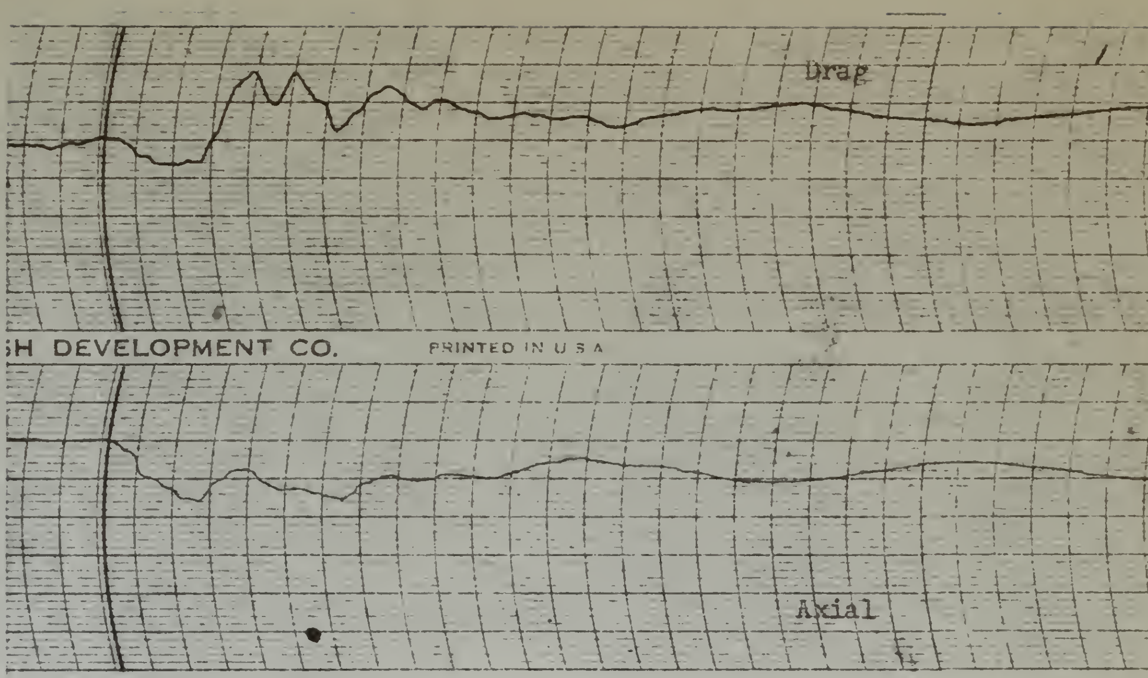

Calibration:

Drag - 1 mm - 220# Cantilever - 1 mm ≐ .375"

Axial - 5 mm = 930# Potentiometer - Refer to Fig. No. 5.

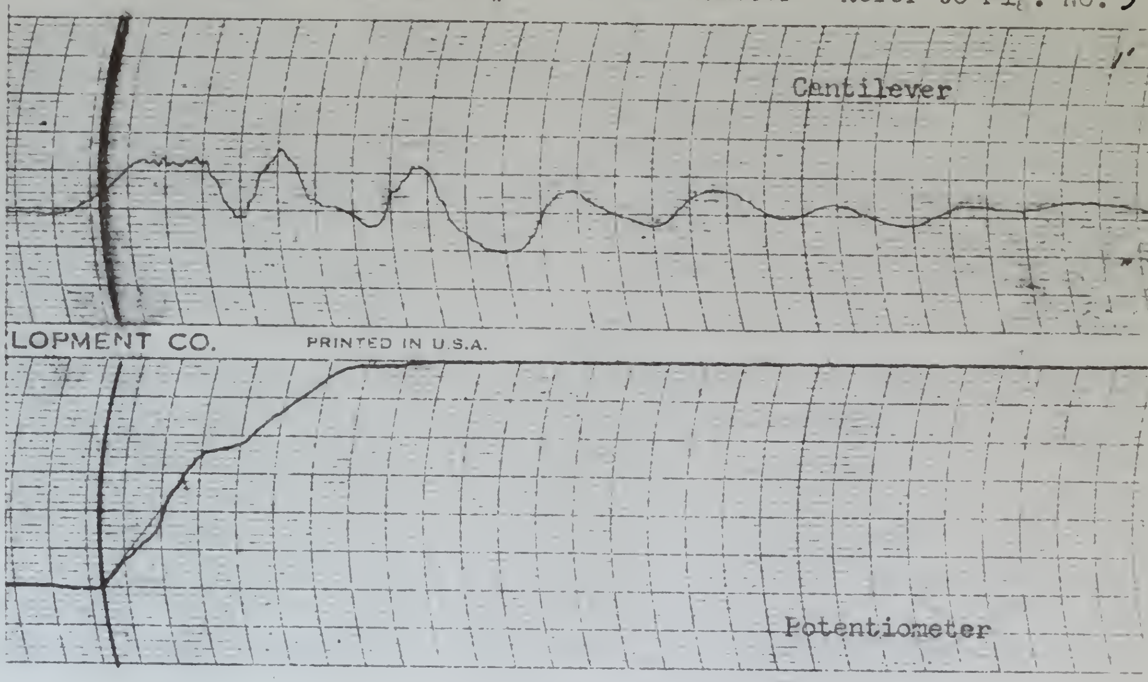

Fig. No. 8

Date: 7/10/49
Strut Angle - 24°
Weight - 1060#
Paper Speed 125 mm/sec

Tire Pressure - 24#
Landing Velocity - 58 FPS
Dropping Velocity - 2 FPS.

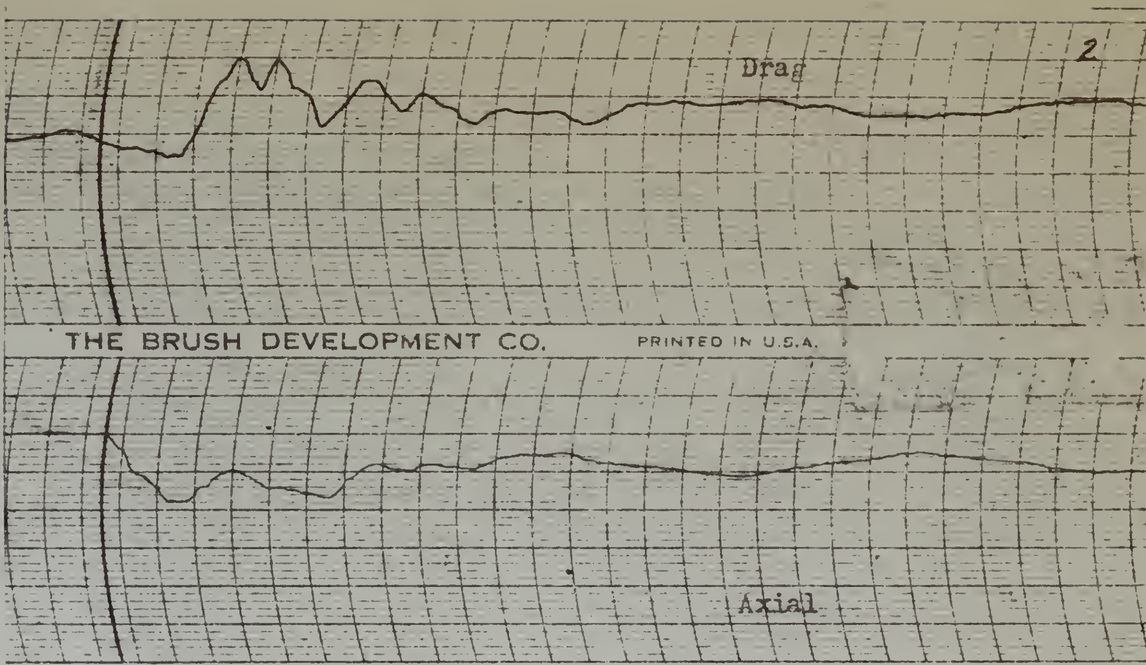

Calibration:

Drag - 1 mm = 220#
Axial - 5 mm = 930#

Cantilever - 1 mm = .375"
Potentiometer - Refer to Fig. No. 5.

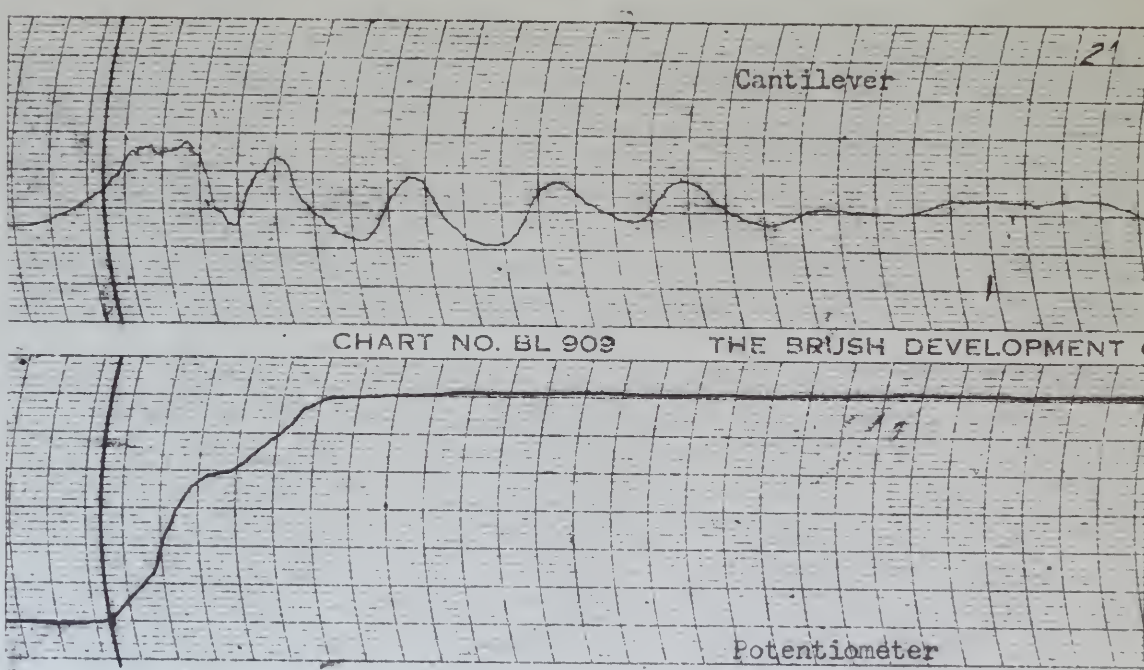

Fig. No. 9

Date: 7/10/49
Strut Angle - 24°
Weight - 1060#
Paper Speed 125 mm/sec

Tire Pressure - 24#
Landing Velocity - 58 FPS
Dropping Velocity - 3 FPS.

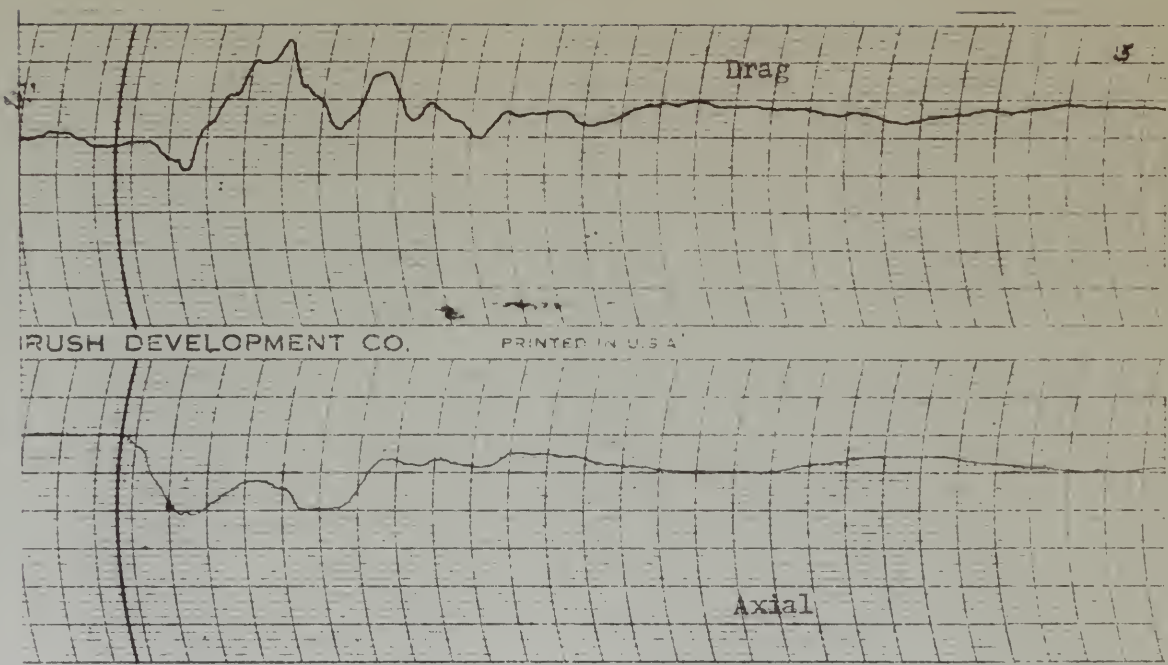

Calibration:
Drag - 1 mm = 220#
Axial - 5 mm = 930#
Cantilever ,- 1 mm = .375"
Potentiometer - Refer **Fig. No. 5.**

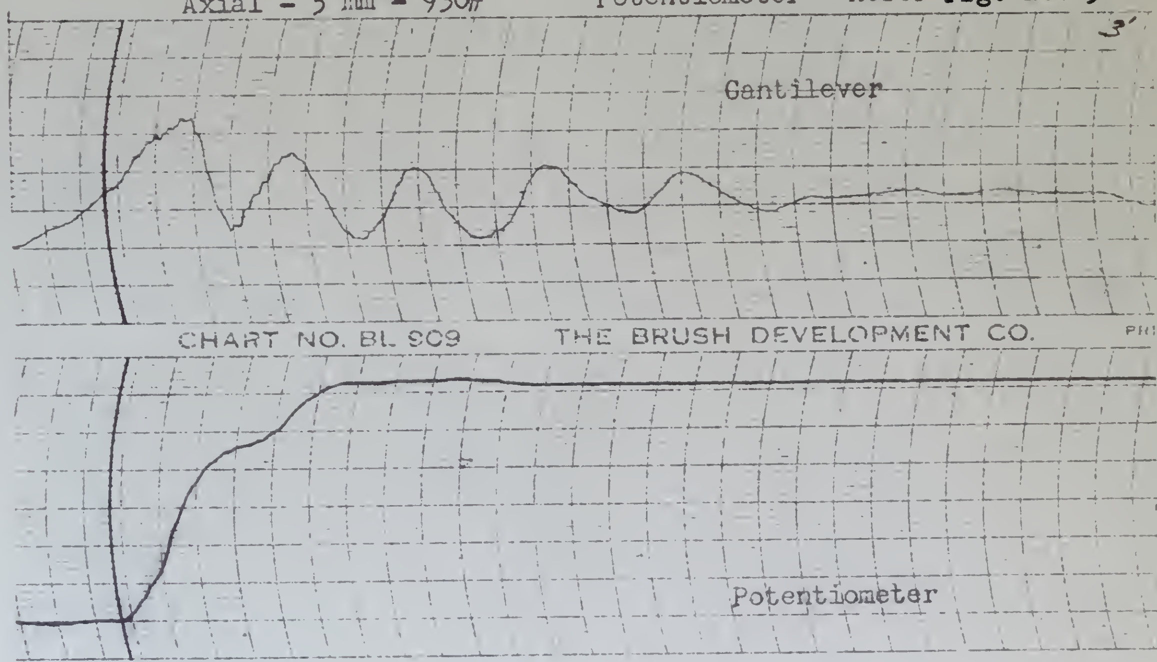

Fig. No. **10**

Date: 7/10/49
Strut Angle - 24°
Weight - 1060#
Brush Speed 125 mm/sec

Tire Pressure - 24#
Landing Velocity - 58 FPS
Dropping Velocity - 4 FPS.

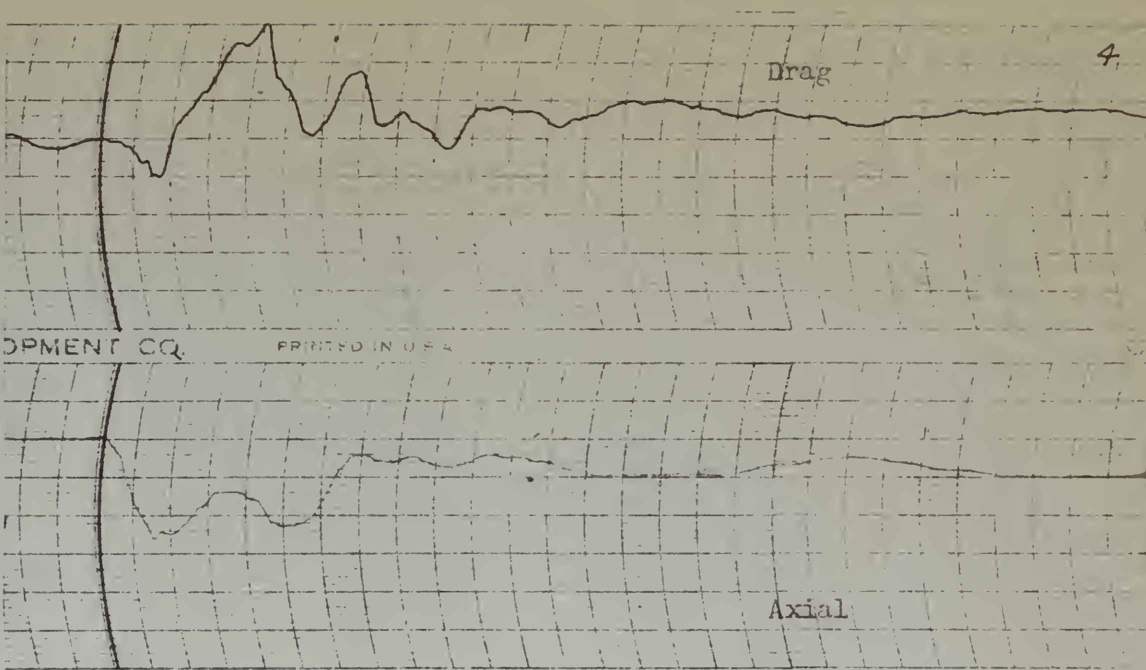

Calibration:

Drag - 1 mm = 220#
Axial - 5 mm = 930#

Cantilever - 1 mm = .375"
Potentiometer - Refer **Fig. No. 5.**

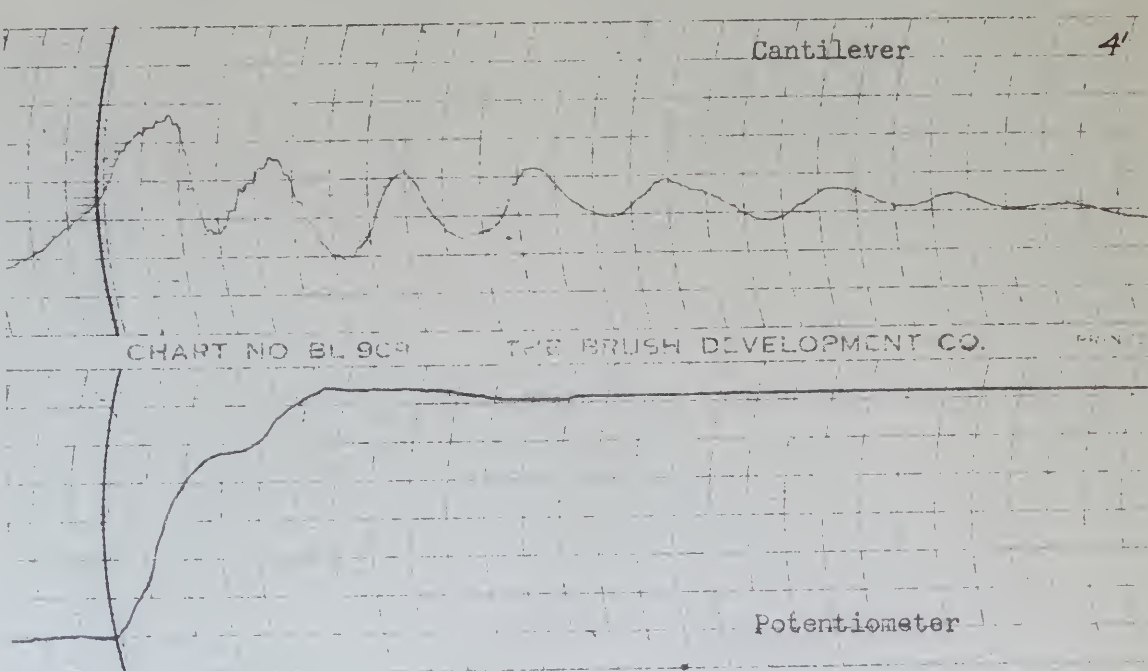

Fig. No. **11**

Date: 7/10/49
Strut Angle - 24°
Weight - 1060#
Brush Speed 125 mm/sec.

Tire Pressure - 24#
Landing Velocity - 58 FPS.
Dropping Velocity - 5 FPS.

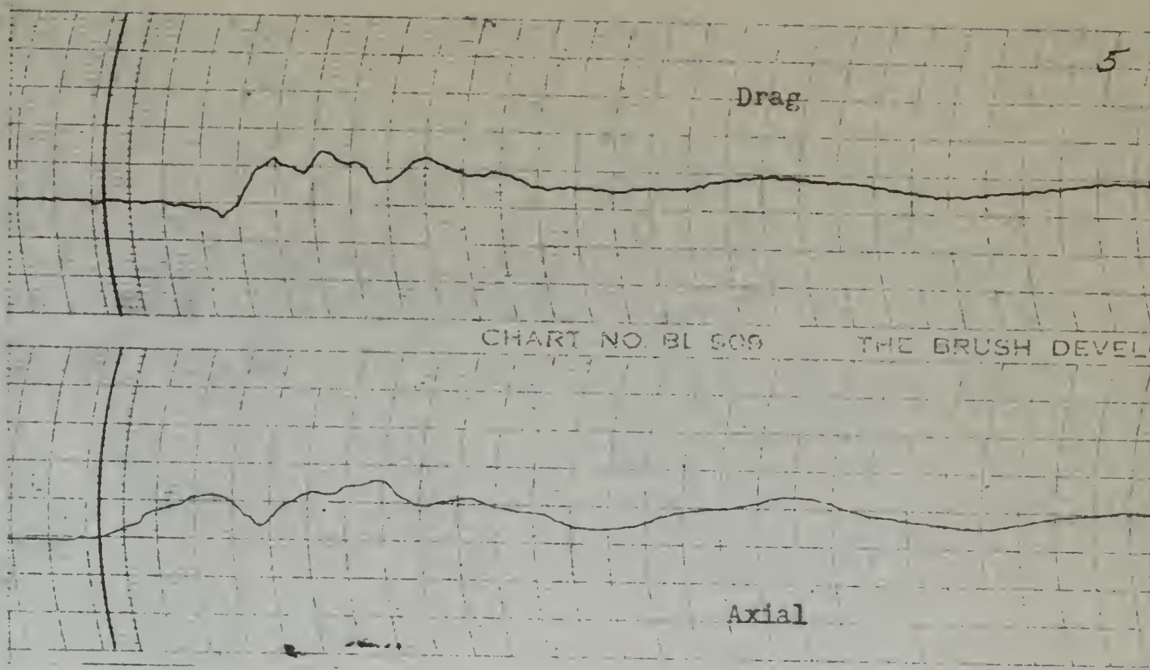

Calibration:
Drag - 1 mm = 110#
Axial - 5 mm = 835#

Cantilever - 1 mm. = .416"
Potentiometer - Refer to Fig. No. 5

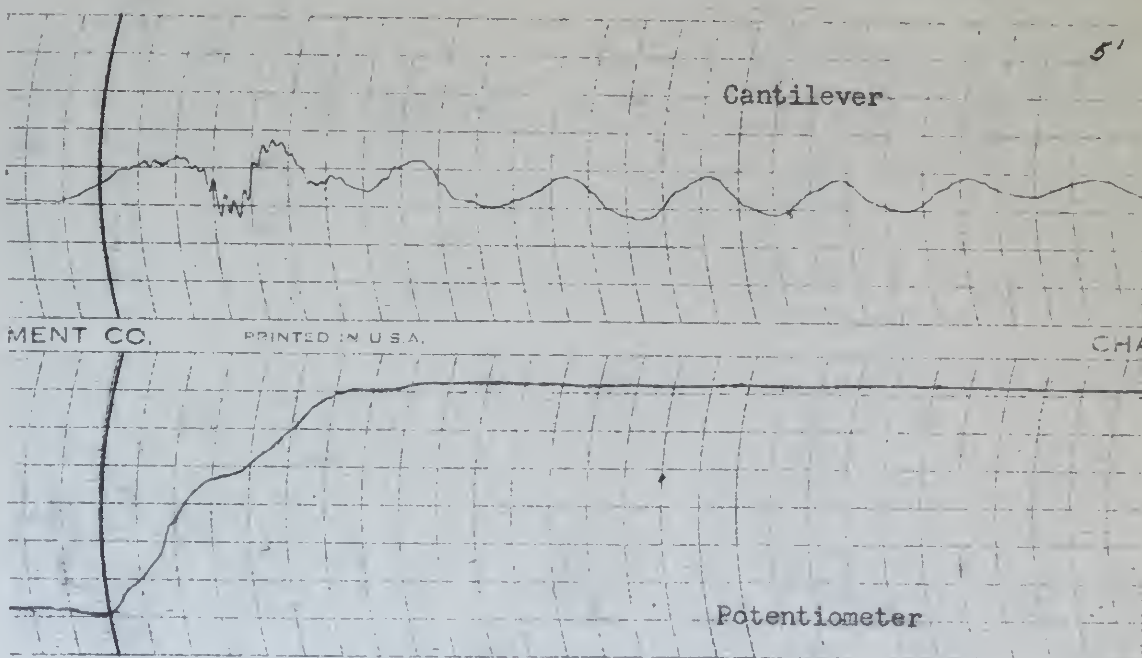

Fig. No. 12

Date: 7/13/49
Strut Angle - 24°
Weight - 1060#
Brush Speed 125 mm/sec.

Tire Pressure - 30#
Landing Velocity - 55.5 FPS
Dropping Velocity - 2 FPS.

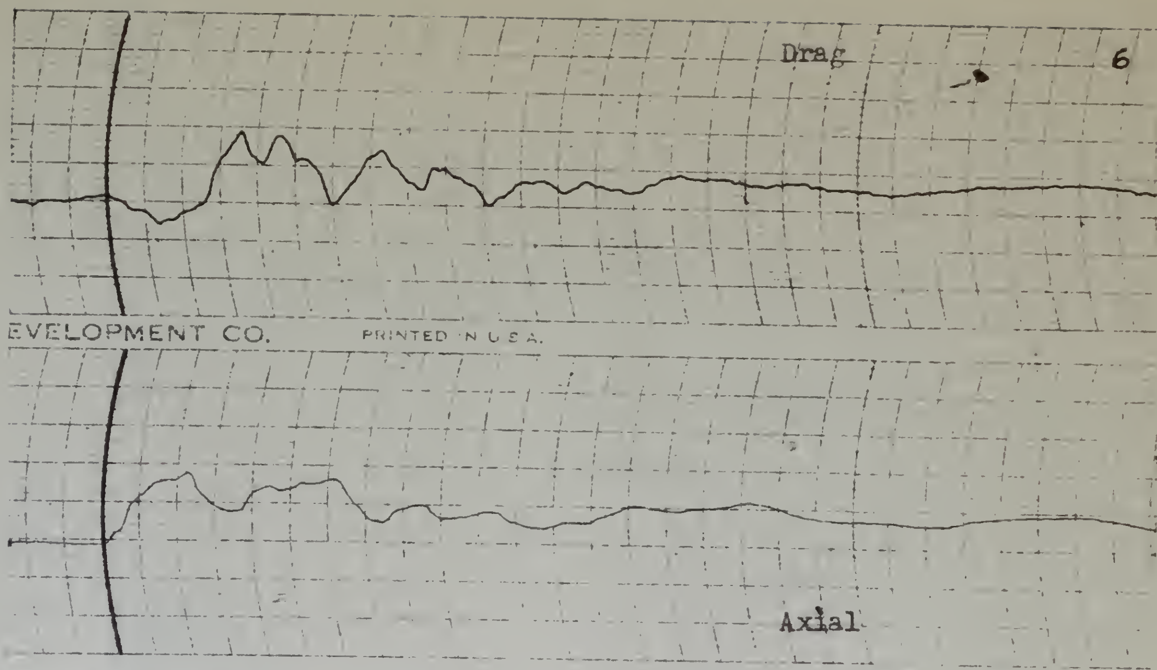

Calibration:
Drag - 1 mm = 110# Cantilever - 1 mm = .416"
Axial - 5 mm = 835# Potentiometer - Refer to Fig. No. 5.

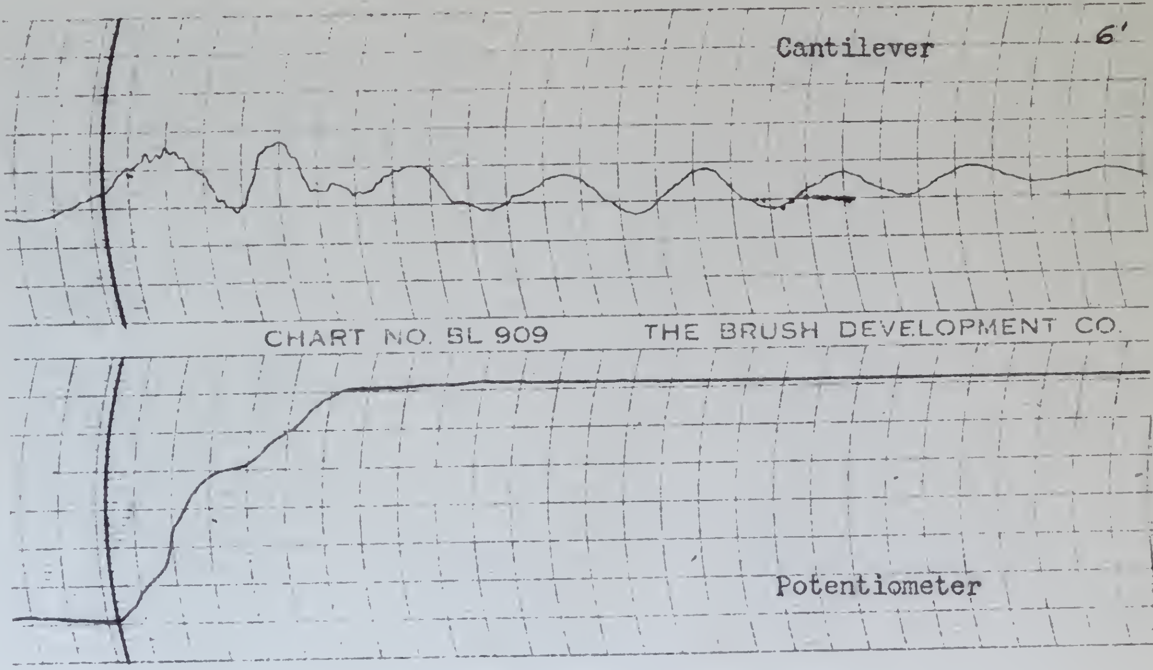

Fig. No. 13

Date: 7/13/49
Strut Angle - 24°
Weight - 1060#
Brush Speed 125 mm/sec.

Tire Pressure - 30#
Landing Velocity - 55.5 FPS.
Dropping Velocity - 3 FPS.

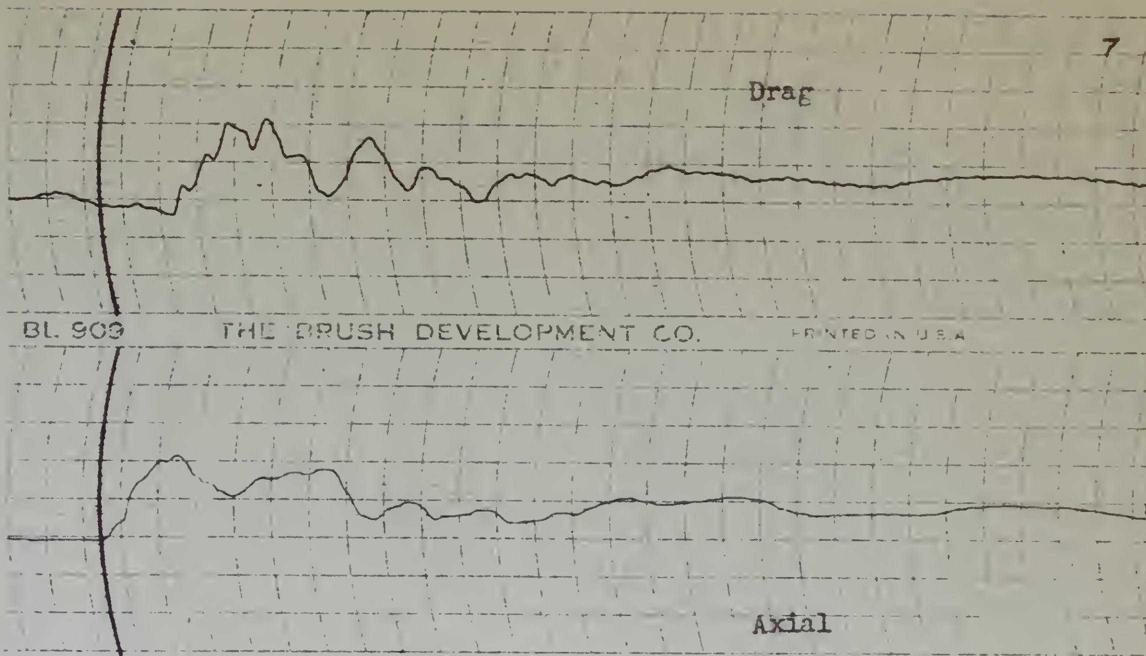

Calibration:
Drag - 1 mm = 110#
Axial - 5 mm = 835#

Cantilever - 1 mm = .416"
Potentiometer - Refer to Fig. No. 5.

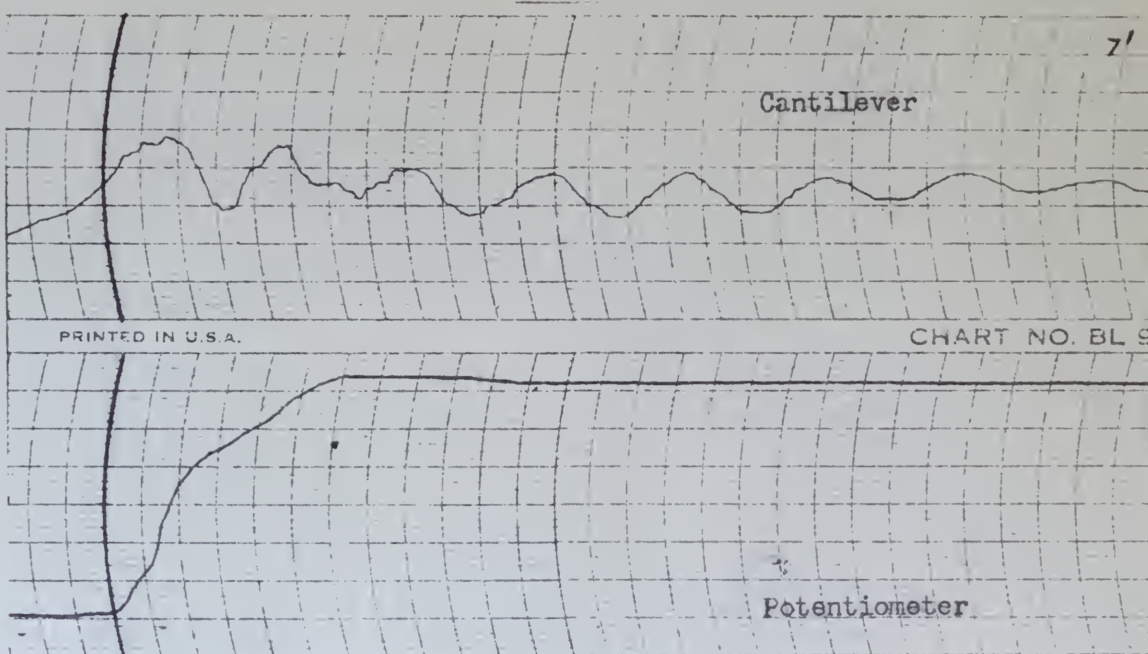

Fig. No. 14

Date: 7/13/49
Strut Angle - 24°
Weight - 1060#
Brush Speed 125 mm/sec.

Tire Pressure - 30#
Landing Velocity - 55.5 FPS
Dropping Velocity - 4 FPS.

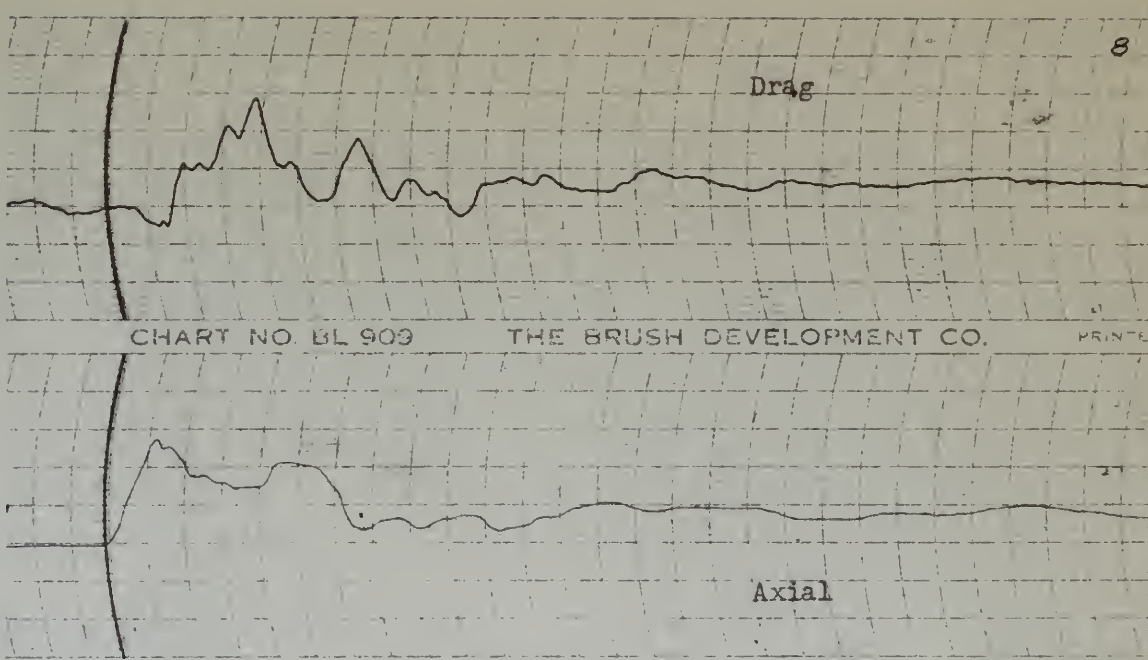

Calibration:
Drag - 1 mm = 110# Cantilever - 1 mm = .416"
Axial - 5 mm = 835# Potentiometer - Refer to Fig. No. 5.

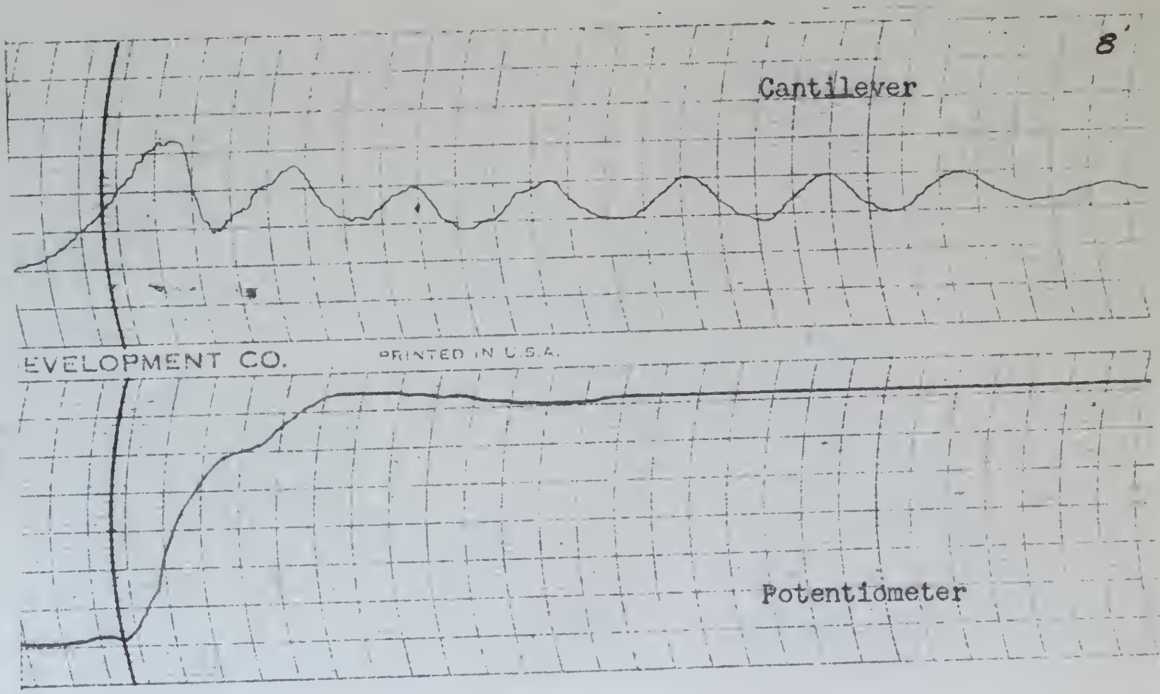

Fig. No. 15

Date: 7/13/49
Strut Angle - 24°
Weight - 1060#
Brush Speed 125 mm/sec.

Tire Pressure - 30#
Landing Velocity - 55.5 FPS
Dropping Velocity - 5 FPS.

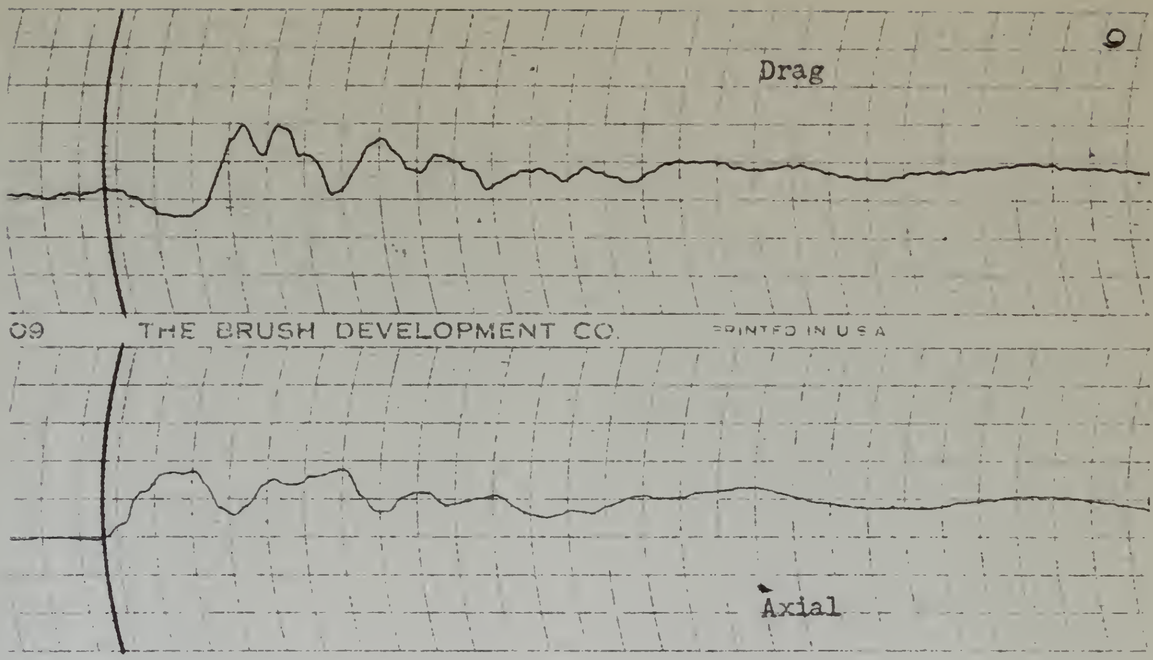

Calibration:

Drag - 1 mm = 110# Cantilever - 1 mm = .416 "

Axial - 5 mm = 835# Potentiometer - Refer to Fig. No. 5.

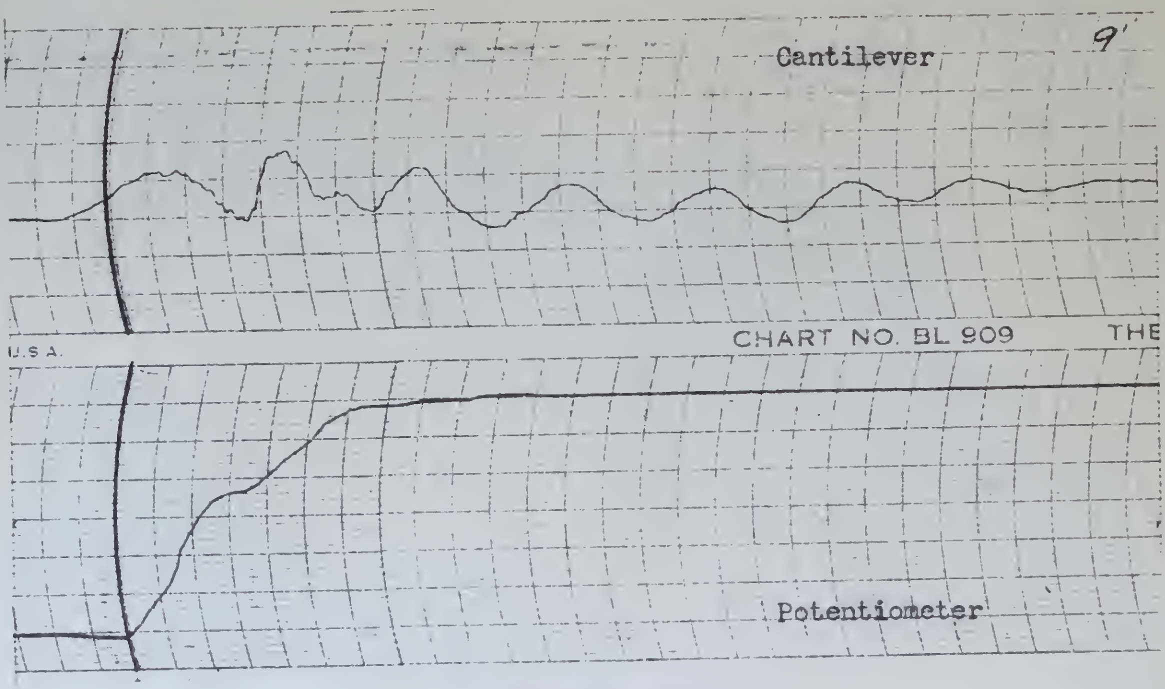

Fig. No. 16

Date: 7/13/49

Strut Angle - 24°

Weight - 1060#

Brush Speed 125 mm/sec

Tire Pressure 35#

Landing Velocity - 56 FPS

Dropping Velocity - 2 FPS.

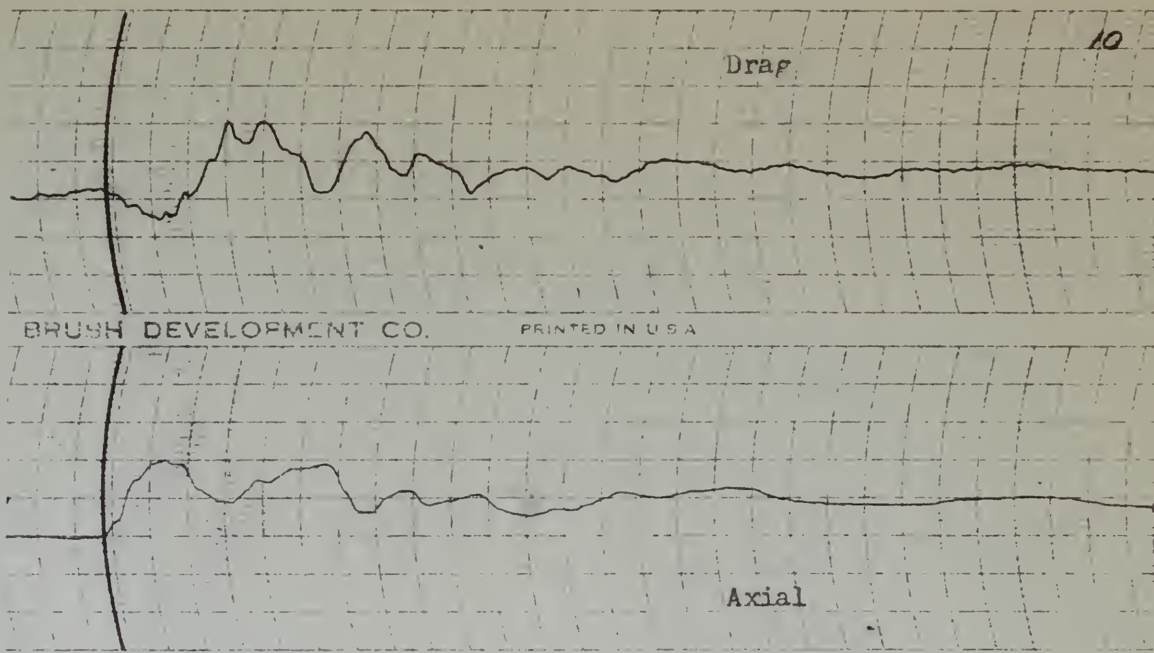

Calibration:

Drag - 1 mm = 110#
Axial - 5 mm = 835#

Cantilever - 1 mm = .416"
Potentiometer - Refer to Fig. No. 5.

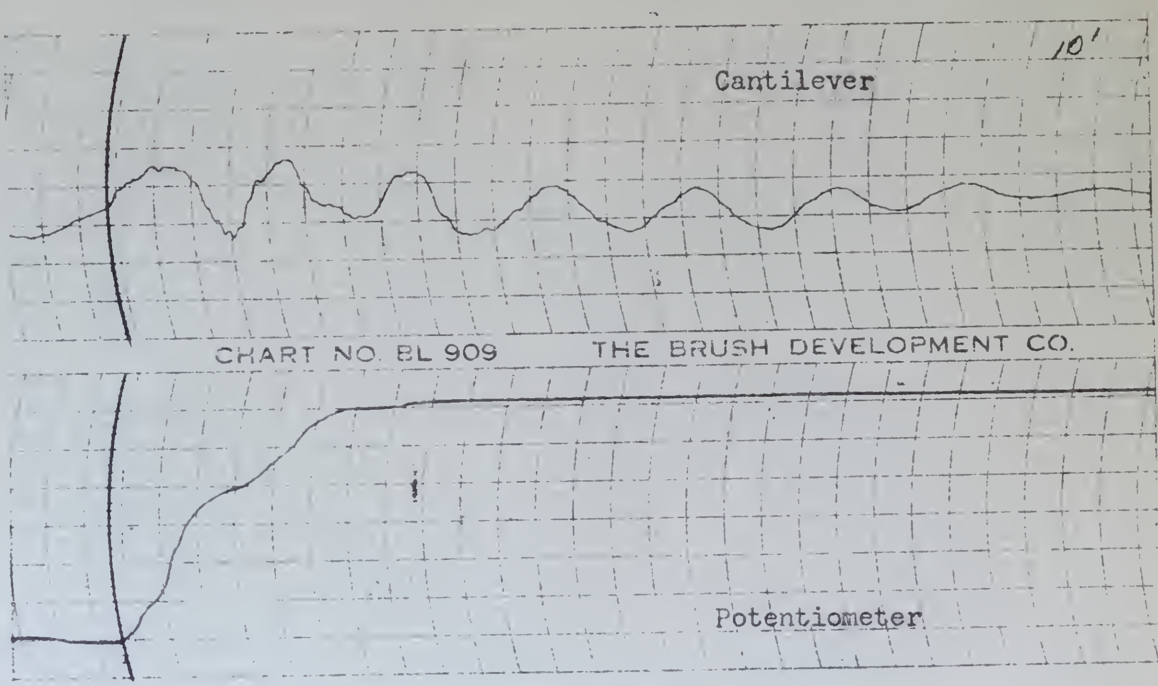

Fig. No. 17

Date: 7/13/49
Strut Angle - 24°
Weight - 1060#
Brush Speed 125 mm/sec.

Tire Pressure 35#
Landing Velocity - 56 FPS
Dropping Velocity - 3 FPS.

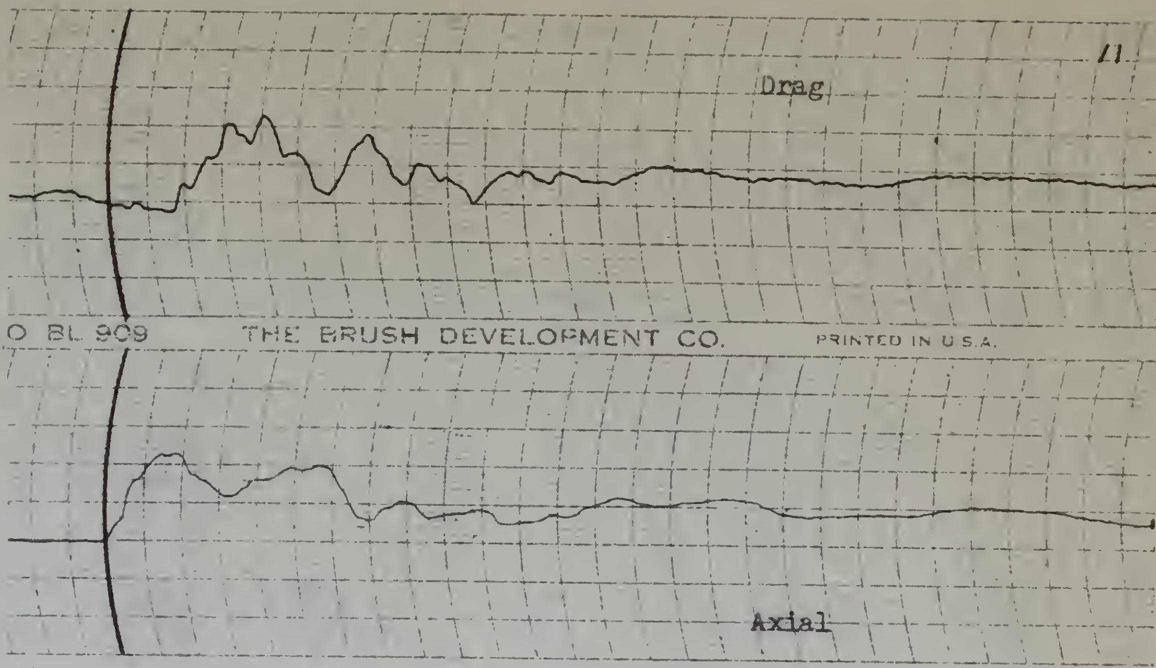

Calibration:

Drag - 1 mm = 110#
Axial - 5 mm = 835#

Cantilever - 1 mm = .416"
Potentiometer - Refer to Fig. No. 5.

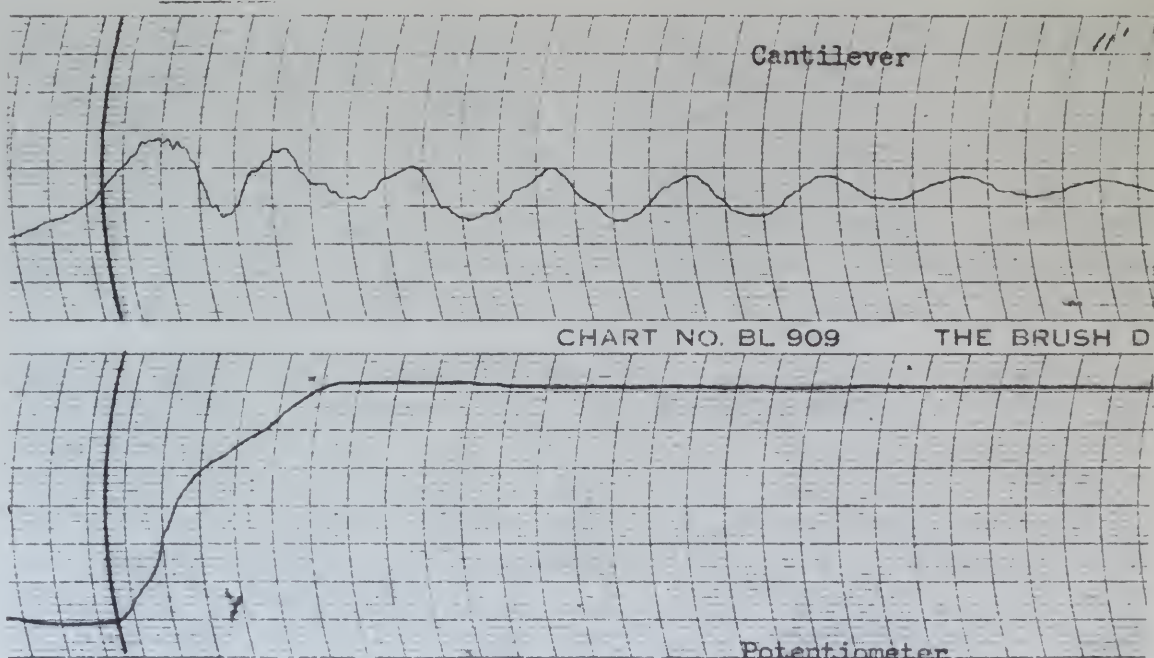

Fig. No. 18

Date: 7/13/49
Strut Angle -24°
Weight - 1060#
Brush Speed 125 mm/sec.

Tire Pressure - 35#
Landing Velocity - 56 FPS
Dropping Velocity - 4 FPS.

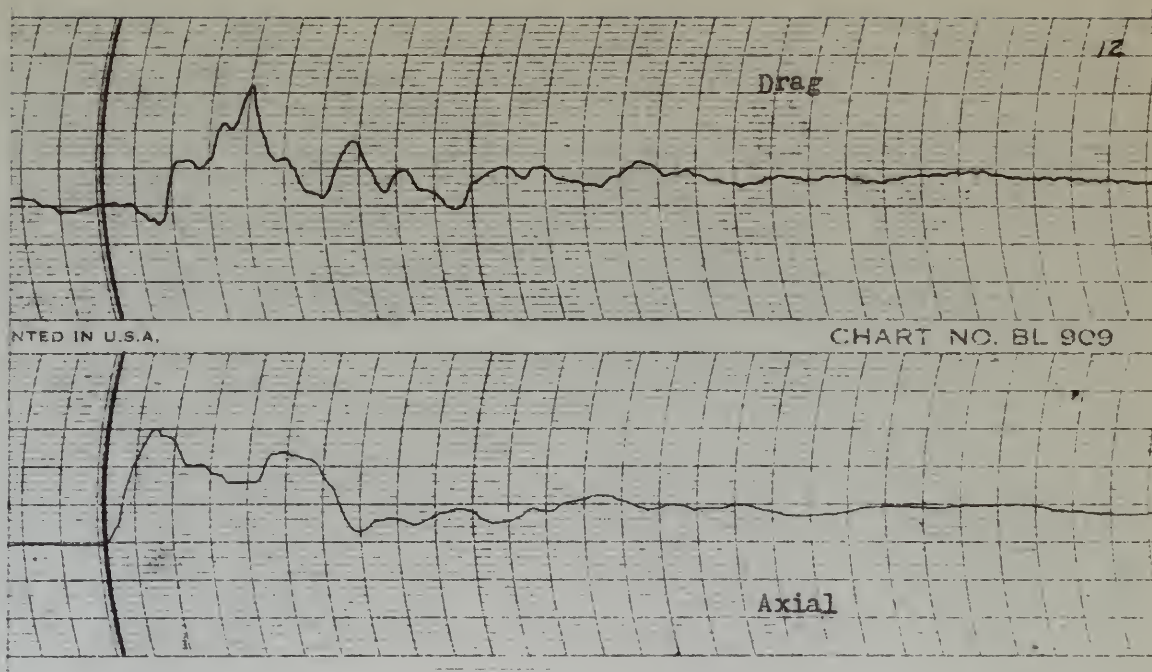

Calibration:

Drag - 1 mm = 110# Cantilever - 1 mm = .416"
Axial - 5 mm = 835# Potentiometer - Refer to Fig. No. 5.

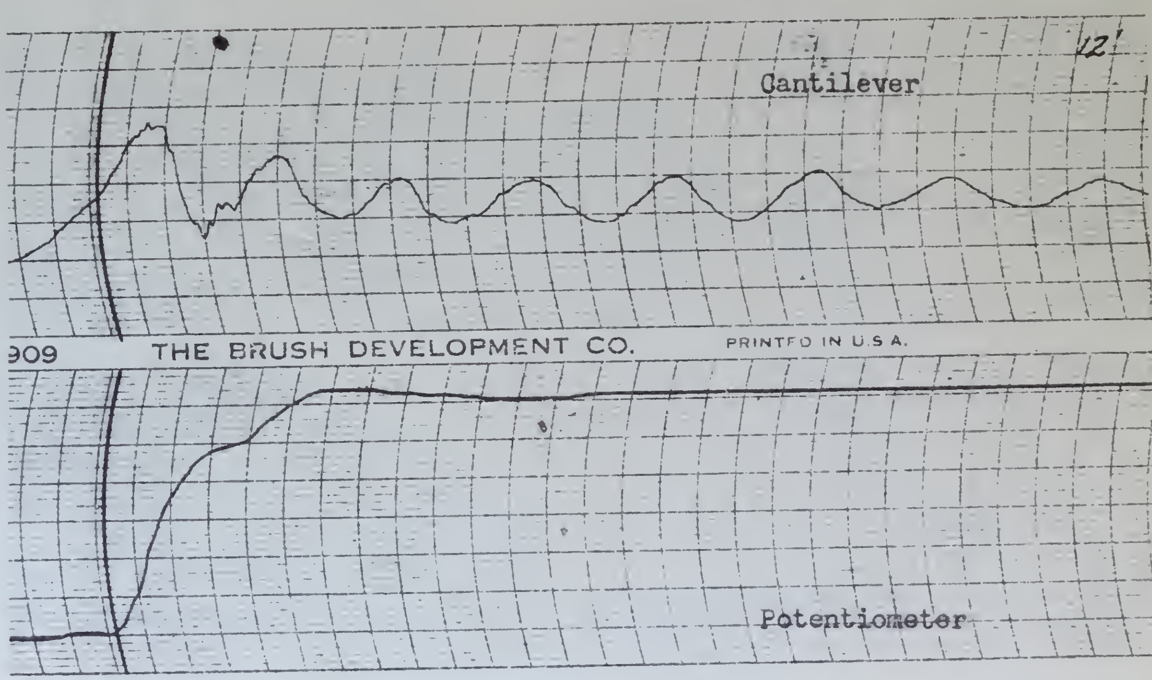

Fig. No. 19

Date: 7/13/49

Strut Angle - 24°
Weight - 1060#
Brush Speed 125 mm/sec.

Tire Pressure - 35#
Landing Velocity - 56 FPS
Dropping Velocity - 5 FPS.

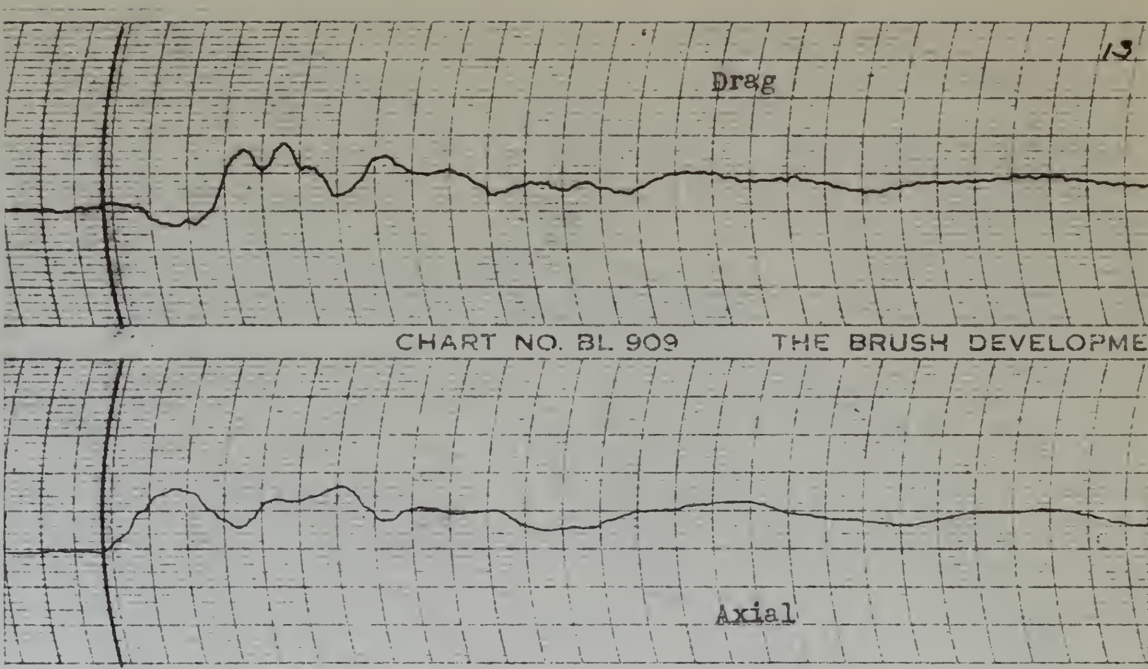

Calibration:
Drag - 1 mm = 110# Cantilever-1 mm = .208"
Axial - 5 mm = 835# Potentiometer - Refer to Fig. No. 5

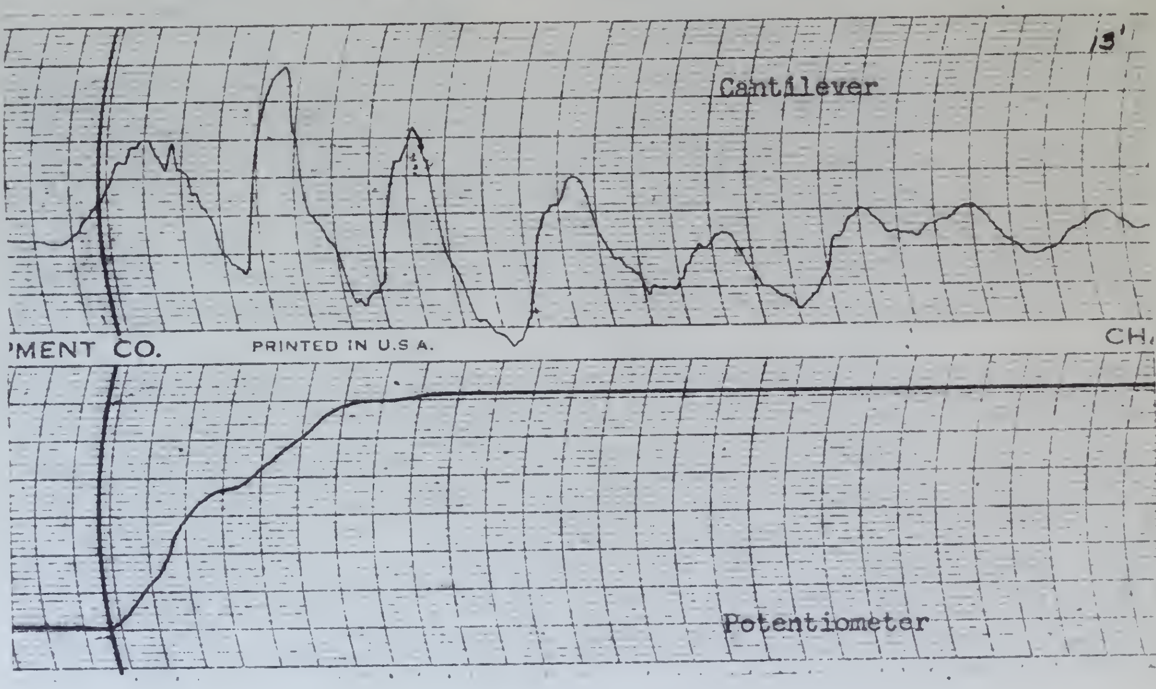

Fig. No. 20

Date: 7/13/49
Strut Angle - 24°
Weight - 1060#
Brush Speed 125 mm/sec.
Tire Pressure - 40#
Landing Velocity - 56 FPS.
Dropping Velocity - 2 FPS.

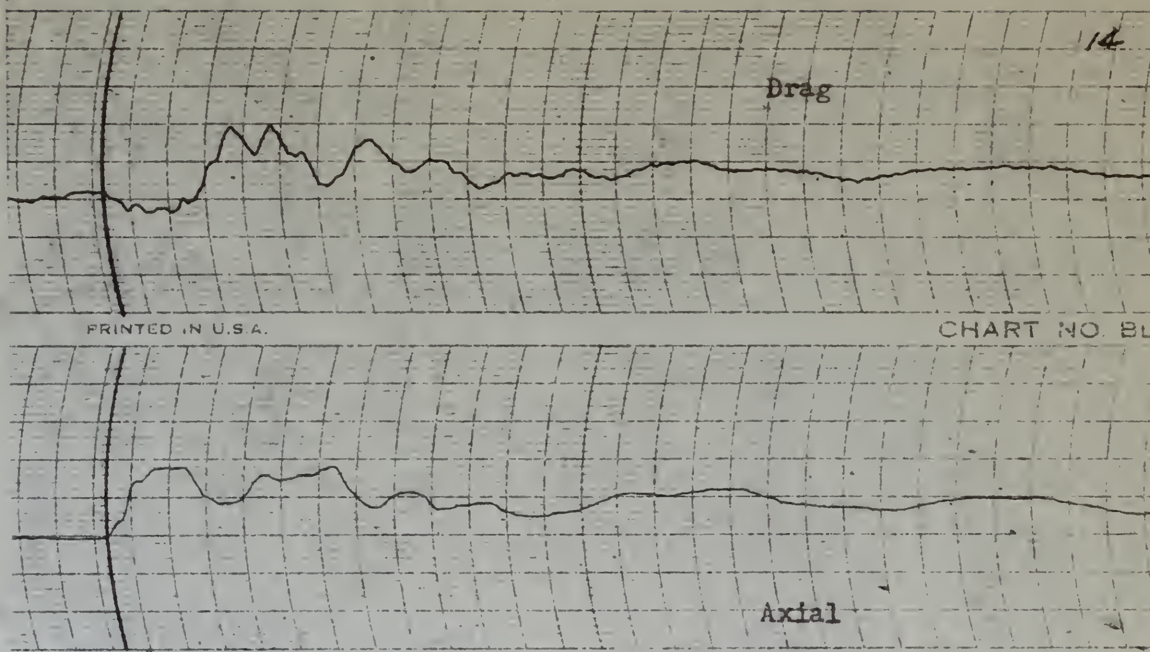

Calibration:

Drag - 1 mm = 110# Cantilever - 1 mm = .208"
Axial - 5 mm = 835# Potentiometer - Refer to Fig. No. 5.

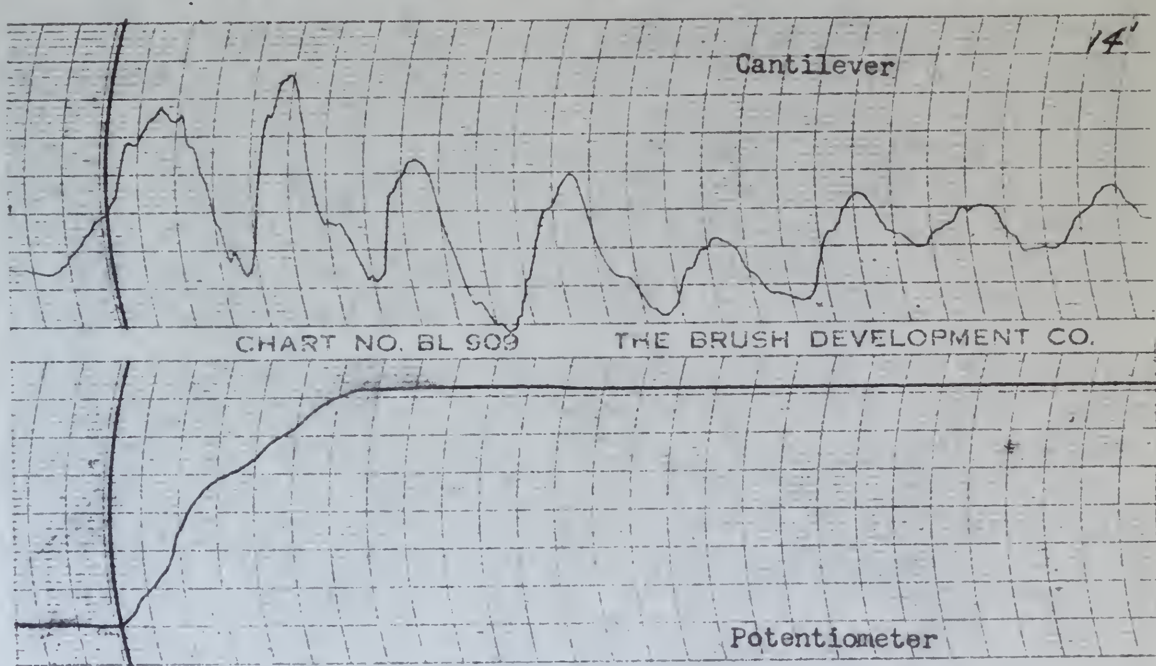

Fig. No. 21

Date: 7/13/49
Strut Angle - 24°
Weight - 1060#
Brush Speed 125 mm/sec

Tire Pressure - 40#
Landing Velocity -56 FPS.
Dropping Velocity - 3 FPS.

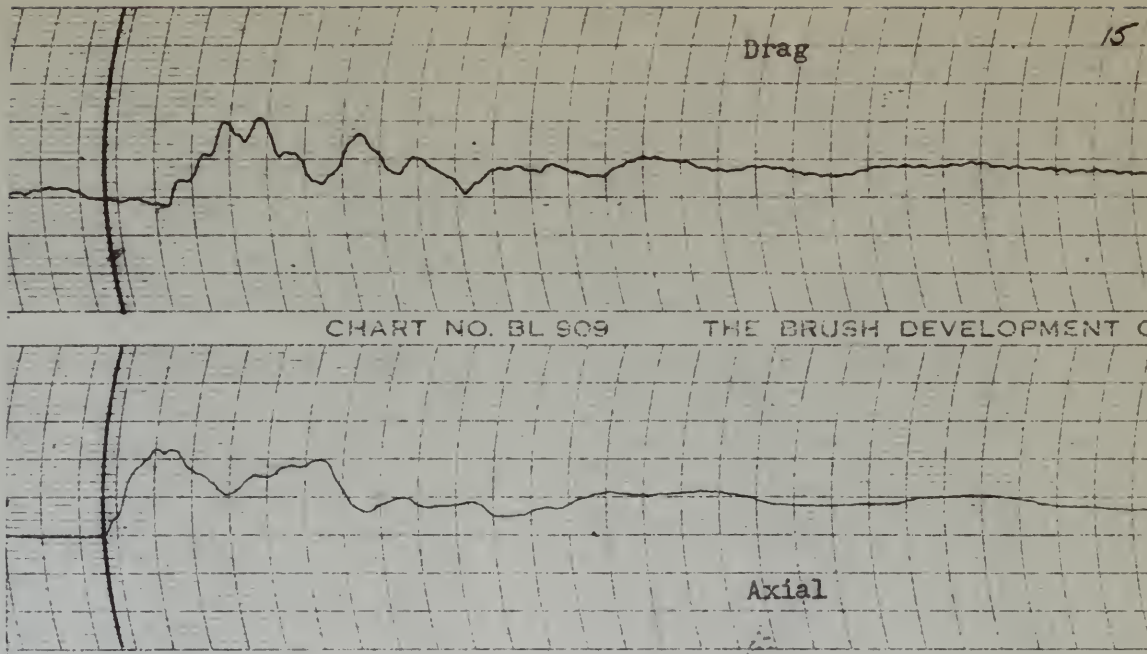

Calibration:

Drag - 1 mm = 110#
Axial - 5 mm = 835#

Cantilever - 1 mm = .208"
Potentiometer - Refer to Fig. No. 5.

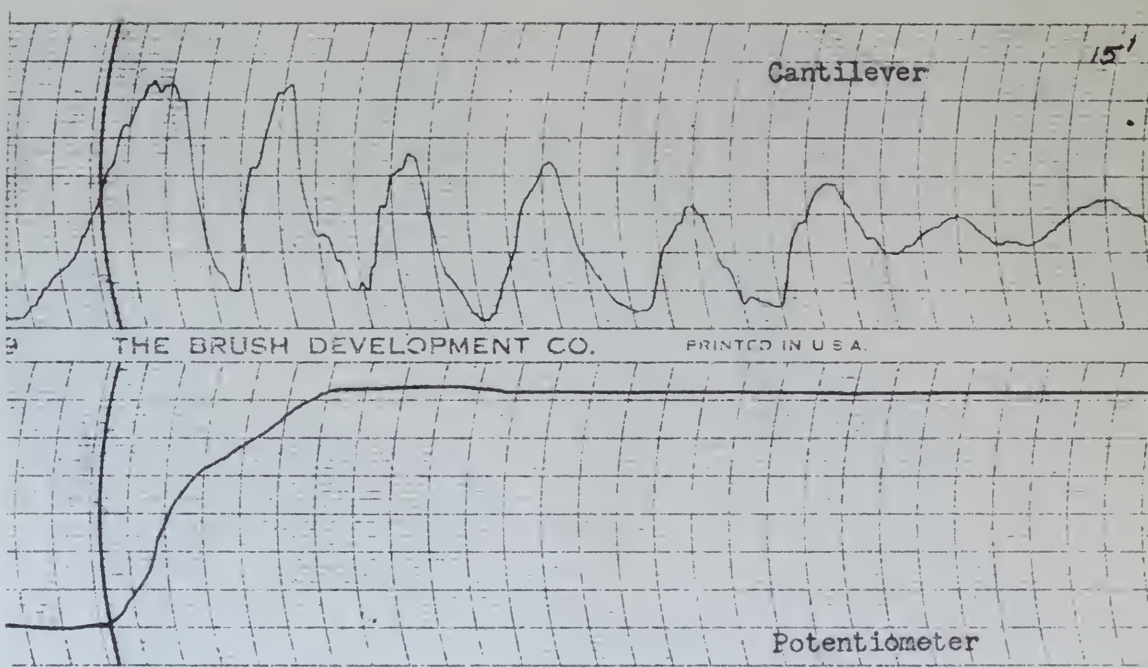

Fig. No. 22

Date: 7/13/49
Strut Angle - 24°
Weight - 1060#
Brush Speed 125 mm/sec.

Tire Pressure - 40#
Landing Velocity - 56 FPS.
Dropping Velocity - 4 FPS.

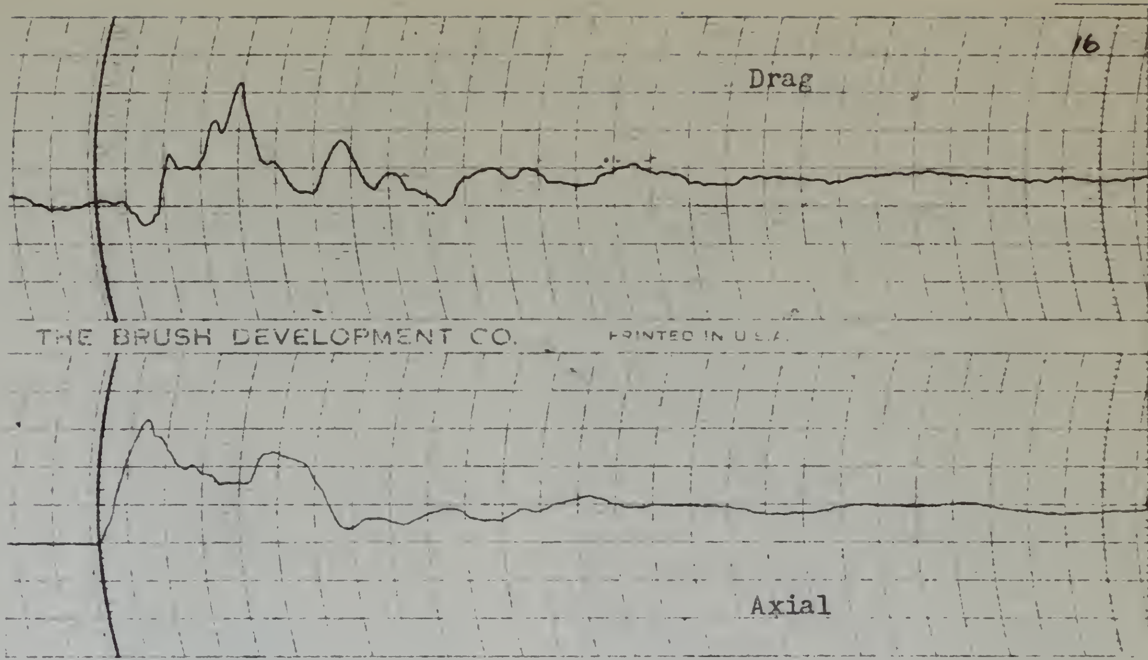

Calibration:
Drag - 1 mm = 110#
Axial - 5 mm = 835#

Cantilever - 1 mm = .208"
Potentiometer - Refer to Fig. No. 5.

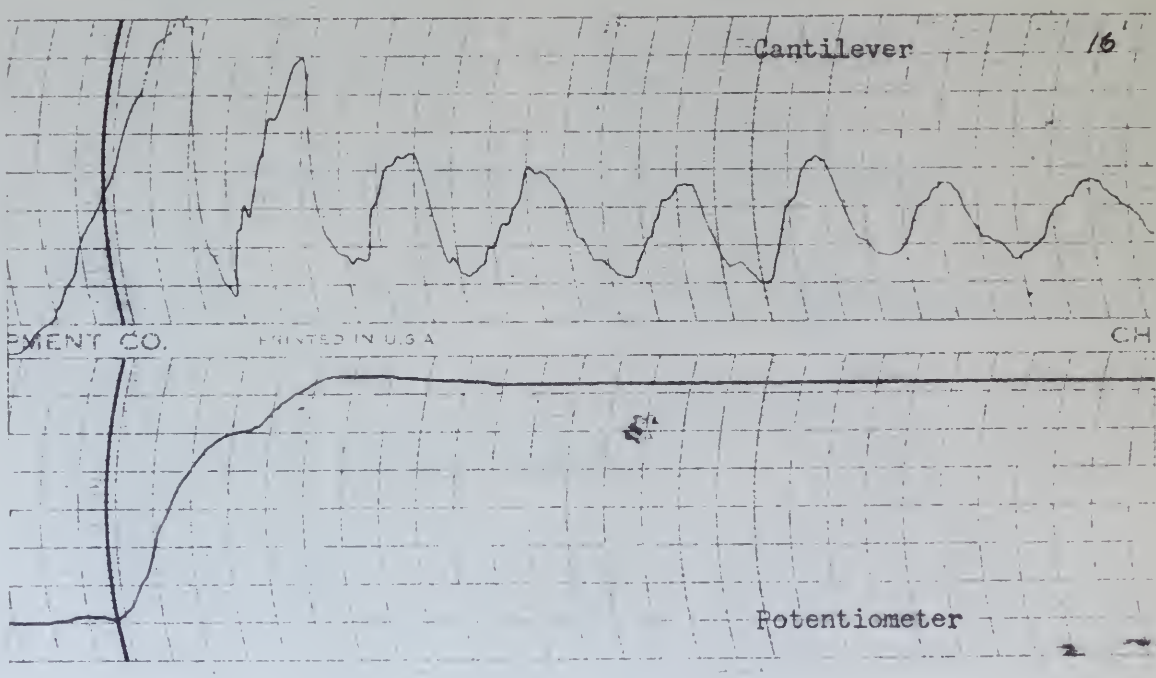

Fig. No. 23

Date: 7/13/49
Strut Angle - 24°
Weight - 1060#
Brush Speed 125 mm/sec.

Tire Pressure - 40#
Landing Velocity - 56 FPS.
Dropping Velocity - 5 FPS.

COMPARISON OF THE TEST AND THEORY

The following problem incorporates the constants computed into the theory developed.

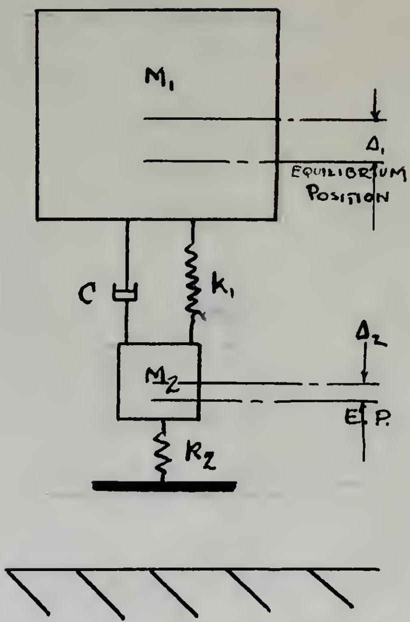

$w_1 = 939$ #

$w_2 = 121$ #

$M_1 = 29.16$ #sec.^{2}/ft.

$M_2 = 3.76$ #sec.^{2}/ft.

$k_{effective} = K_{measured} \cos 24^{\circ}$

$k_1 = 1584$ #/ft.

$k_{2_{eff}} = 11280$ #/ft.

$-\Delta_1 = -.094$ ft.

$k_{2_{meas}} = 12300$ #/ft.

$-\Delta_2 = -.636$ ft.

DETERMINATION OF (C) DAMPING CONSTANT

Example:

From Fig. No. 14 at $t = .04$ sec.

$$\dot{x} = \frac{dx}{dt} = \frac{1.07}{.04} = 26.8 \text{ ft./sec.}$$

$$K_1 = 69 \text{ \#/in.}$$

$$F = \frac{9.5}{5} \times 835 \text{ \#} = 1615 \text{ \#}$$

Oleo Deflection = 1.07 inches

$$F = C\dot{x} + K_1 x$$

$$1615 = C26.8 + 69 \times 1.07$$

$$C = \frac{1549}{26.8} = 57.5 \text{ \#sec./in.}$$

$$C = 688 \text{ \#sec./ft.}$$

$C_{ave.} = \underline{\underline{653}}$

Equations of Motion

$$-M_1 \ddot{x}_1 - C(\dot{x}_1 - \dot{x}_2) - k_1(x_1 - x_2) = 0$$

$$-M_2 \ddot{x}_2 - k_2 x_2 + k_1(x_1 - x_2) + C(\dot{x}_1 - \dot{x}_2) = 0$$

Or

$$S^4 + 196S^3 + 3{,}475.65S^2 + 67{,}182.05S + 162{,}965.34 = 0$$

By Synthetic Division

$S_1 = -2.759$

$S_2 = 178.62$

$S_3 = -7.31 - i\ 16.65$

$S_4 = -7.31 + i\ 16.65$

$A = \phi_1 A'$ $\quad$ $A = -50.03A'$

$B = \phi_2 B'$ $\quad$ $B = -.141B'$

$C = \phi_3 C'$ $\quad$ $C = .663 + i\ .862$

$D = \phi_4 D'$ $\quad$ $D = .663 - i\ .862$

$A' = \frac{E_1}{E}$; $B' = \frac{E_2}{E}$; $C' = \frac{E_3}{E}$; $D' = \frac{E_4}{E}$

$E = i\ 286{,}359.82$; $\quad$ $A' = .00745$;

$E_1 = i\ 2133.98$; $\quad$ $B' = -.01699$;

$E_2 = -i\ 4866.03$; $\quad$ $C' = -.052 + i\ .112$;

$E_3 = -32.145 - i\ 14.91$ $\quad$ $D' = -.052 - i\ .112$;

$E_4 = +32.145 - i\ 14.91$ $\quad$ $A = -.373$

$B = .0024$;

$$C = -.131 + i\ .029;$$

$$D = -.131 - i\ .029;$$

$$x_1 = -.373e^{-2.759t} + .0024e^{-178.62t} + e^{-7.31t}\,(-.262 \cos.\ 16.65t + .058 \sin 16.65t)$$

$$x_2 = .00745e^{-2759t} - .01699e^{-178.62t} + e^{-7.31}\,(-.104 \cos.\ 16.65t + .224 \sin 16.65t)$$

Frequency,

$$f = \frac{\omega}{2\pi} = \frac{1}{2\pi}\sqrt{16.65} = \frac{4.09}{2\pi} = .651 \text{ CPS}$$

Period of Vibration,

$$T = \frac{2\pi}{\omega} = \frac{6.28}{16.65} = .377 \text{ sec.}$$

There is a close agreement between the test data and the theory. The computed period of vibration is .377 seconds whereas the experimental period is .388 seconds. The theory is within 2.8 per cent of the experimental values. The theoretical maximum force for the landing gear's dropping velocity of four feet per second shows an axial force of 2440 pounds. An experimental force, 1910 pounds, was indicated on the Brush recorder. The association between these two values is not as close as that of the period previously mentioned. The affinity between the maximum theoretical force is 22 per cent greater than in the experimental axial load.

From Fig. Nos. 6 & 7 are chosen the values of spring constant used in the illustrated problem. These values are not true constants, but are assumed to be in order to simplify computations. For example, as the air compressed in the oleo, the force versus distance curve was not of a linear relation. This was also true for the tire. In other words, these "spring constants" are not in reality, constant. Had they been a true constant the agreement between the theoretical and experimental would have been closer.

There is a close agreement between the test data and the theory. The computed period of vibration is .377 seconds whereas the experimental period is .388 seconds. The theory is within 3.5 per cent of the experimental values. The theoretical maximum force for the landing gear's sinking velocity of four feet per second shows an axial force of 2250 pounds. An experimental force, 1910 pounds, was indicated on the Brush recorder. The correlation between these two values is not as close as that of the period previously mentioned. The difference between the maximum theoretical force is 17 per cent greater than is the experimental axial load.

From Fig. Nos. 6 & 7 are chosen the values of spring constant used in the illustrated problem. These values are not true constants, but are assumed to be in order to simplify computations. For example, as the air compressed in the oleo, the force versus distance curve was not of a linear relation. This was also true for the tire. In other words, these "spring constants" are not in reality, constant. Had they been a true constant the agreement between the theoretical and experimental would have been closer.

$x_2 = .007\,e^{-2.759t} - .017e^{-178.62t} + e^{-7.13t}\,(-.104\cos 16.65t + .224\sin 16.65t)$

t	(C) cos ω	sin ω	$e^{-7.31t}$	(E) -.104C	(F) +.224D	(E+F)	x_2
.0	1	0	1	-.1040	0	-.1040	-.1040
.01	.986	.165	.929	-.1036	.0370	-.0666	-.0656
.02	.945	.326	.863	-.0982	.0730	-.0252	-.0218
.03	.878	.479	.802	-.0912	.1072	+.0160	+.0128
.04	.786	.617	.747	-.0818	.1382	+.0564	+.0422
.05	.675	.738	.695	-.0702	.1654	+.0952	+.0661
.06	.540	.841	.644	-.0561	.1886	+.1322	+.0852
.07	.390	.921	.600	-.0406	.2062	+.1652	+.0992
.08	.239	.971	.557	-.0205	.2180	+.1875	+.1043
.09	.071	.997	.516	-.0073	.2235	+.2162	+.1118
.10	-.091	.996	.481	+.0095	.2235	+.2320	+.1117
.11	-.257	.967	.447	+.0278	.2170	+.2448	+.1095
.12	-.416	.909	.416	+.0432	.2035	+.2467	+.1025
.13	-.555	.830	.387	+.0576	.1860	+.2436	+.0941
.14	-.690	.725	.360	+.0716	.1625	+.2341	+.0844
.15	-.801	.598	.336	+.0833	.1340	+.2173	+.0731
.16	-.887	.468	.310	+.0922	.1050	+.1972	+.0611
.17	-.925	.302	.289	+.0990	.0681	+.1671	+.0483
.18	-.990	.140	.268	+.1030	.0314	+.1344	+.0347
.19	-.999	-.018	.249	+.1039	-.0040	+.0999	+.0249
.20	-.984	-.190	.232	+.1024	-.0425	+.0599	+.0139
.21	-.936	-.345	.215	+.0972	-.0786	+.0186	+.0043
.22	-.862	-.494	.200	+.0900	-.1110	-.0210	-.0042

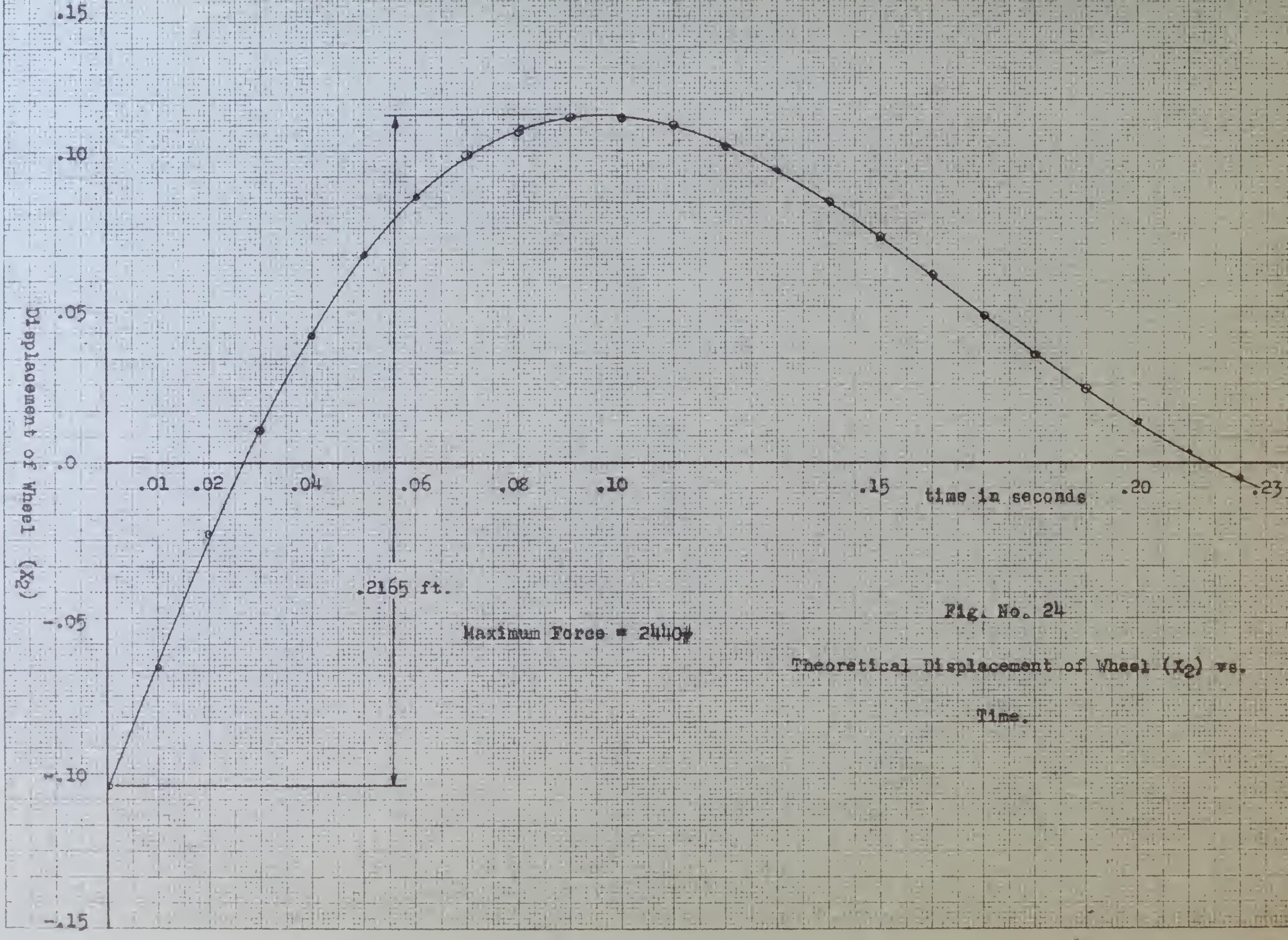

Fig. No. 24

Theoretical Displacement of Wheel (X_2) vs. Time.

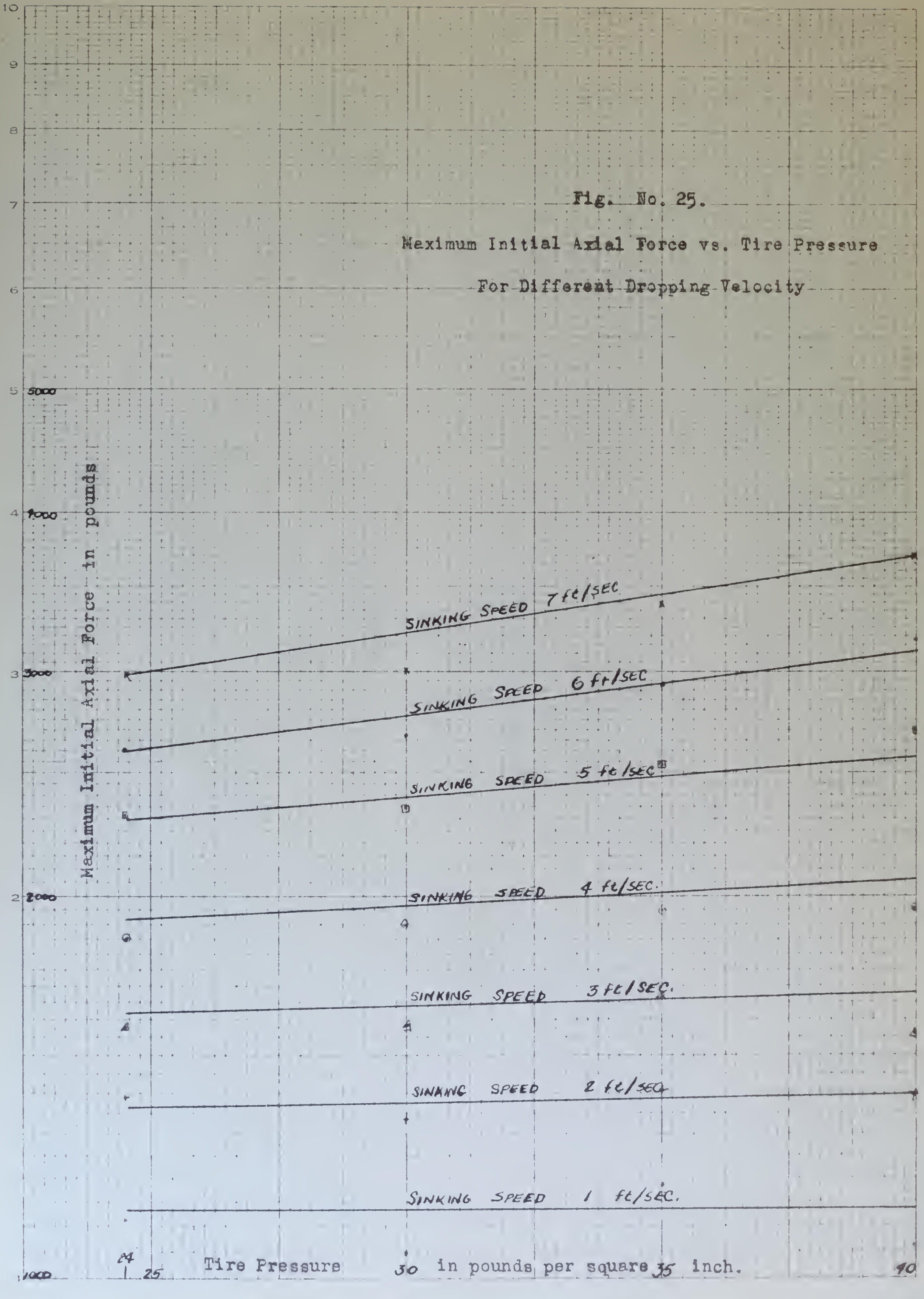
Fig. No. 25.
Maximum Initial Axial Force vs. Tire Pressure
For Different Dropping Velocity
Maximum Initial Axial Force in pounds
5000
4000
3000
2000
1000
SINKING SPEED 7 ft/SEC
SINKING SPEED 6 ft/SEC
SINKING SPEED 5 ft/SEC
SINKING SPEED 4 ft/SEC.
SINKING SPEED 3 ft/SEC.
SINKING SPEED 2 ft/SEC
SINKING SPEED 1 ft/SEC.
24
25
30
35
40
Tire Pressure in pounds per square inch.

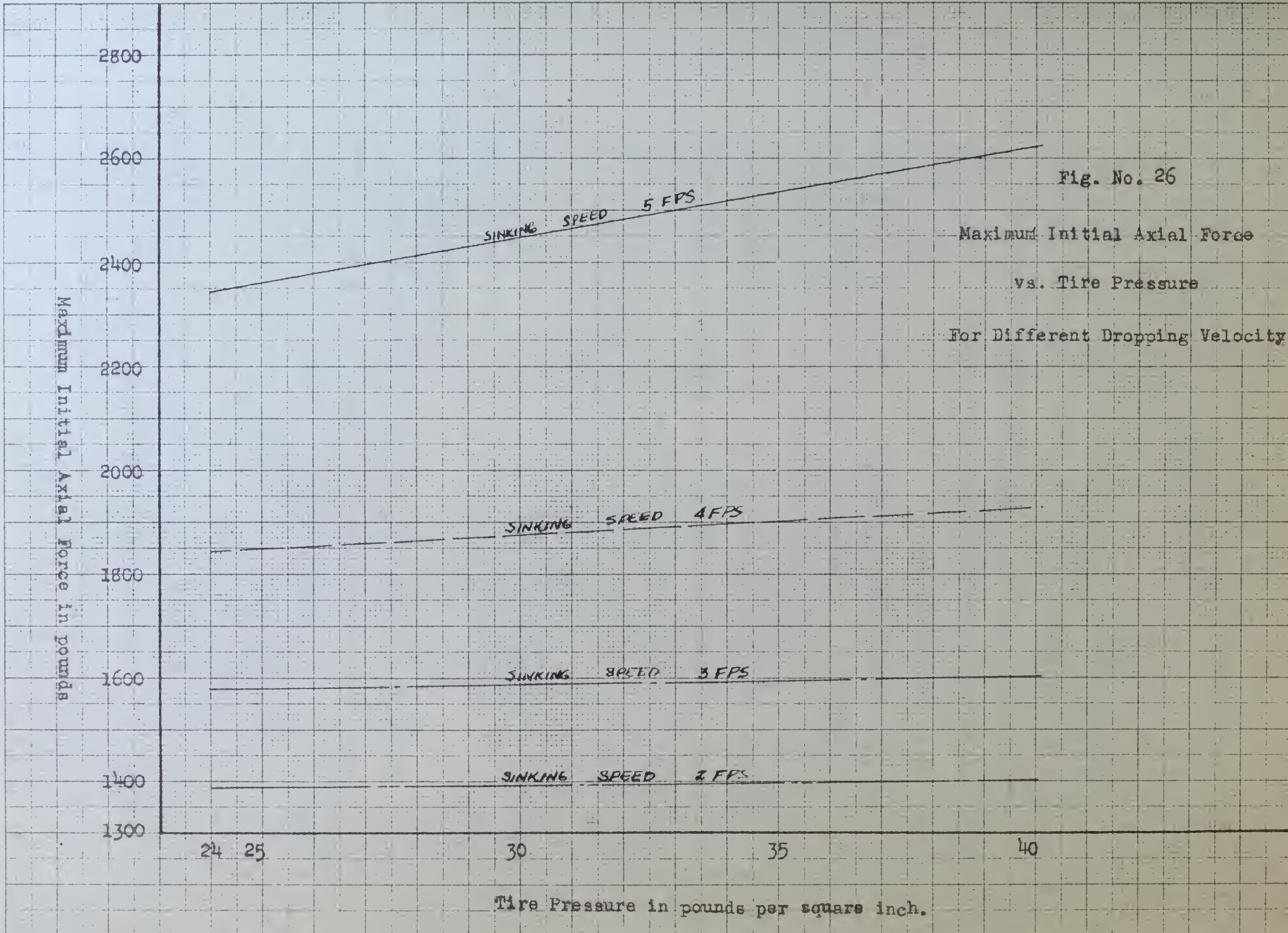

Fig. No. 26

Maximum Initial Axial Force

vs. Tire Pressure

For Different Dropping Velocity.

CONCLUSION

The data of this experiment indicates that the theory and the experimental results agree quite closely.

As the tire pressure increases the axial force increases. At the slower striking velocities the effect of the tire pressure is not as noticeable as when the vertical forces are of a greater magnitude. In Fig. No. 25 there is an indication that the axial force increases by the square as the dropping velocity increases linearly. On log paper (Fig. No. 25) the graph shows equal distances between the curves at constant tire pressure. These equal distances increase between the curves as the pressure of the tire becomes greater. This gives an increasing slope. Fig. No. 26 shows a better picture of this slope and indicates more clearly that as the tire pressure increases the force along the strut increases.

Both the Brush Recorder and motion picture show that a temporary frequency is introduced into the system during the first phase of landing impact of the landing gear. This frequency results from the drag forces imposed on the strut, and the vertical vibrations of the tire. The film indicates that the landing gear, after its initial contact with the flywheel, does not leave the landing surface.

CONCLUSION

The data of this experiment indicates that the theory and the experimental results agree quite closely.

As the tire pressure increases the axial force increases. At the slower striking velocities the effect of the tire pressure is not as noticeable as when the vertical forces are of a greater magnitude. In Fig. No. 25 there is an indication that the axial force increases by the square as the dropping velocity increases linearly. On log paper (Fig. No. 25) the graph shows equal distances between the curves at constant tire pressure. These equal distances increase between the curves as the pressure of the tire becomes greater. This gives an increasing slope. Fig. No. 26 shows a better picture of this slope and indicates more clearly that as the tire pressure increases the force along the strut increases.

Both the brush Recorder and motion picture show that a temporary frequency is introduced into the system during the first phase of landing impact of the landing gear. This frequency results from the drag forces imposed on the strut, and the vertical vibrations of the tire. The film indicates that the landing gear, after its initial contact with the flywheel, does not leave the landing surface.

The theoretical and experimental development points out that critical damping for the oleo had been reached.

It is recommended that a more complete study be made of the "spring constants", damping characteristics, and dynamic friction involved in the problem of landing gear.

APPENDIX

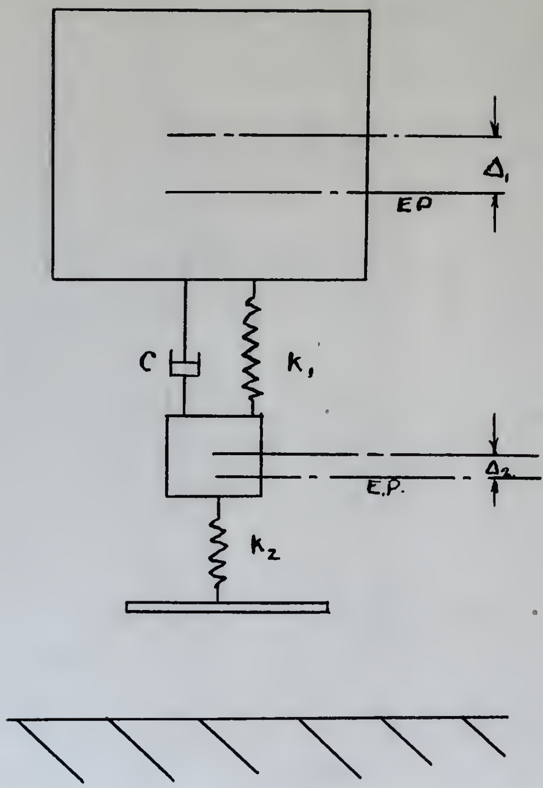

k_1 = spring constant of Oleo strut

k_2 = spring constant of tire

C = damping constant of oleo strut

W_1 = weight of airplane

W_2 = weight of wheel and lower half of strut

M = mass

A, B, C, D, A', B', C', D' = constants

i = imaginary unit

s = complex frequency

From the forces acting on this diagram the equation of motion can be written.

$$(1) \quad -m_1\ddot{x}_1 - c(\dot{x}_1 - \dot{x}_2) - k_1(x_1 - x_2) = 0$$

$$(2) \quad -m_2\ddot{x}_2 - k_2x_2 + k_1(x_1 - x_2) + c(\dot{x}_1 - \dot{x}_2) = 0$$

Let: $x_1 = Ae^{st}$ $\quad \dot{x}_1 = SAe^{st}$ $\quad \ddot{x}_1 = S^2Ae^{st}$

$x_2 = Be^{st}$ $\quad \dot{x}_2 = sBe^{st}$ $\quad \ddot{x}_2 = s^2Be^{st}$

Subs. in (1) and (2) the following results

$$(3) \quad (-m_1s^2 - cs - k_1)Ae^{st} + Be^{st}(cs + k_1) = 0$$

$$(4) \quad (-m_2s^2 - cs - k_1 - k_2)Be^{st} + Ae^{st}(cs + k_1) = 0$$

The e^{st} cancels--Then putting into determinant form and solve for s (which is the freq.)

$$\begin{vmatrix} -m_1 s^2 - cs - k_1 & Cs + k_1 \\ cs + k_1 & -m_2 s^2 - cs - k_1 - k_2 \end{vmatrix} = 0 \qquad \begin{matrix}(5)\\(6)\end{matrix}$$

Solve the resultant equation

$$(7) \quad m_1 m_2 s^4 + (m_1 + m_2) c s^3 + (k_1 m_1 + k_1 m_2 + k_2 m_1) s^2 + k_2 c s + k_1 k_2 = 0$$

Letting $a = \dfrac{(m_1 + m_2)\, c}{m_1 m_2}$

$b = \dfrac{k_1 m_1 + k_1 m_2 + k_2 m_1}{m_1 m_2}$

$c = \dfrac{k_2 c}{m_1 m_2}$

$d = \dfrac{k_1 k_2}{m_1 m_2}$

$$(8) \quad s^4 + a s^3 + b s^2 + c s + d = 0$$

Brots "approximate factorization" gives a relative close solution for this equation under certain conditions:

$$f(s) \cong (s^2 + as + b)\left(s^2 + \frac{c}{b}s + \frac{d}{b}\right) = 0$$

$$(9) \quad s_{1,2} \cong \frac{-a \pm \sqrt{a^2 - 4b}}{2}$$

$$(10) \quad s_{3,4} \cong \frac{-\frac{c}{b} \pm \sqrt{\left(\frac{c}{b}\right)^2 - 4\frac{d}{b}}}{2}$$

Synthetic division give better results. With this, the following can be written:

$$(11)\quad x_1 = Ae^{s_1t} + Be^{s_2t} + Ce^{s_3t} + De^{s_4t}$$

$$(12)\quad x_2 = A'e^{s_1t} + B'e^{s_2t} + C'e^{s_3t} + D'e^{s_4t}$$

Then put A in terms of A'

$$\begin{vmatrix} (-m_1s^2 - cs - k_1)A & + & (Cs + k_1)A' \\ (cs + k_1)A & + & (-m_2s^2 - c_s - k_1 - k_2)A' \end{vmatrix} = 0$$

or

$$(13)\quad A = \frac{cs_1 + k_1}{m_1s_1^2 + cs_1 + k_1} A' = \varnothing_1 A'$$

$$(14)\quad B = \frac{cs_2 + k_1}{m_1s_2^2 + cs_2 + k_1} B' = \varnothing_2 B'$$

$$(15)\quad C = \frac{cs_3 + k_1}{m_1s_3^2 + cs_3 + k_1} C' = \varnothing_3 C'$$

$$(16)\quad D = \frac{cs_4 + k_1}{m_1s_4^2 + cs_4 + k_1} D' = \varnothing_4 D'$$

Now set up boundary conditions

at $t = 0$ $\quad x_1 = -\Delta_1 \qquad x_2 = -\Delta_2$

$\qquad\qquad\quad \dot{x}_1 = vo \qquad \dot{x}_2 = vo$

where $-\Delta_1$ and $-\Delta_2$ equal the distance from center of mass to equilibrium position

$$-\ _1 = \frac{(m_1 - m_2)\ g}{K_1} + \frac{(m_1 + m_2)\ g}{K_2}$$

$$-\Delta_2 = \frac{(m_1 + m_2)\, g}{K_2}$$

(17) $-\Delta_1 = Ae^{s_1 t} + Be^{s_2 t} + Ce^{s_3 t} + De^{s_4 t}$

(18) $-\Delta_2 = A'e^{s_1 t} + B'e^{s_2 t} + C'e^{s_3 t} + D'e^{s_4 t}$

Let V_o = The dropping velocity of the landing gear and taking derivative, gives

(19) $V_o = S_1 Ae^{s_1 t} + S_2 Be^{s_2 t} + S_3 Ce^{s_3 t} + S_4 De^{s_4 t}$

(20) $V_o = S_1 A'e^{s_1 t} + S_2 B'e^{s_2 t} + S_3 C'e^{s_3 t} + S_4 D'e^{s_4 t}$

Rewriting (17) and (19)

(21) $-\Delta_1 = \phi_1 A'e^{s_1 t} + \phi_2 B'e^{s_2 t} + \phi_3 C'e^{s_3 t} + \phi_4 D'e^{s_4 t}$

(22) $V_o = S_1\phi_1 A'e^{s_1 t} + S_2\phi_2 B'e^{s_2 t} + S_3\phi_3 C'e^{s_3 t} + S_4\phi_4 D'e^{s_4 t}$

Here are four equations, four unknowns putting in determinant form:

$$\text{Let } E = \begin{vmatrix} 1 & 1 & 1 & 1 \\ \phi_1 & \phi_2 & \phi_3 & \phi_4 \\ S_1 & S_2 & S_3 & S_4 \\ S_1\phi_1 & S_2\phi_2 & S_3\phi_3 & S_4\phi_4 \end{vmatrix}$$

$$E_1 = \begin{vmatrix} -\Delta_2 & 1 & 1 & 1 \\ -\Delta_1 & \phi_2 & \phi_3 & \phi_4 \\ V_o & S_2 & S_3 & S_4 \\ V_o & S_2\phi_2 & S_3\phi_3 & S_4\phi_4 \end{vmatrix} ; \quad E_2 = \begin{vmatrix} 1 & -\Delta_2 & 1 & 1 \\ \phi_1 & -\Delta_2 & \phi_3 & \phi_4 \\ S_1 & V_o & S_3 & S_4 \\ S_1\phi_1 & V_o & S_3\phi_3 & S_4\phi_4 \end{vmatrix}$$

$$E_3 = \begin{vmatrix} 1 & 1 & -\Delta_2 & 1 \\ \phi_1 & \phi_2 & -\Delta_1 & \phi_4 \\ s_1 & s_2 & V_o & s_4 \\ s_1\phi_1 & s_2\phi_2 & V_o & s_4\phi_4 \end{vmatrix} ; \quad E_4 = \begin{vmatrix} 1 & 1 & 1 & -\Delta_2 \\ \phi_1 & \phi_2 & \phi_3 & -\Delta_1 \\ s_1 & s_2 & s_3 & V_o \\ s_1\phi_1 & s_2\phi_2 & s_3\phi_3 & V_o \end{vmatrix}$$

Therefore:

$$A' = \frac{E_1}{E} ; \; B' = \frac{E_2}{E} ; \; C' = \frac{E_3}{E} ; \; D' = \frac{E_4}{E}$$

Substituting in (11) and (12) the equations of motion result.

$$(23) \quad x_1 = \frac{E_1}{E} \phi_1 e^{s_1 t} + \frac{E_2}{E} \phi_2 e^{s_2 t} + \frac{E_3}{E} \phi_3 e^{s_3 t} + \frac{E_4}{E} \phi_4 e^{s_4 t}$$

$$(24) \quad x_2 = \frac{E_1}{E} e^{s_1 t} + \frac{E_2}{E} e^{s_2 t} + \frac{E_3}{E} e^{s_3 t} + \frac{E_4}{E} e^{s_4 t}$$

Let s_1, s_2, s_3, and s_4 be complex roots,

Or,

$s_1 = a_1 + i\omega_1$ $\qquad$ $s_3 = a_2 + i\omega_2$

$s_2 = a_1 - i\omega_1$ $\qquad$ $s_4 = a_2 - i\omega_2$

Again (11) and (12) can be written

$$(25) \quad x_1 = Ae^{(a_1 + i\omega_1)t} + Be^{(a_1 - i\omega_1)t} + Ce^{(a_2 + i\omega_2)t} + De^{(a_2 - i\omega_2)t}$$

$$(26) \quad x_2 = A'e^{(a_1 + i\omega_1)t} + B'e^{(a_1 - i\omega_1)t} + C'e^{(a_2 + i\omega_2)t} + D'e^{(a_2 - i\omega_2)t}$$

DeMoivre's Theorem:

$$e^{i\omega t} = \cos \omega t + i \sin \omega t$$

$$e^{-i\omega t} = \cos \omega t - i \sin \omega t$$

(25) and (26) are written:

$$(27) \quad x_1 = Ae^{at}e^{+i\omega_1 t} + Be^{a_1 t}e^{-i\omega_1 t} + Ce^{a_2 t}e^{+i\omega_2 t} + De^{a_2 t}e^{-i\omega_2 t}$$

$$(28) \quad x_2 = A'e^{a_1 t}e^{+i\omega_1 t} + B'e^{a_1 t}e^{-i\omega_1 t} + C'e^{a_2 t} e^{+i\omega_2 t} + D'e^{a_2 t}e^{-i\omega_2 t}$$

$$(29) \quad x_1 = (A \cos \omega_1 t + Ai \sin \omega_1 t)\, e^{a_1 t} + e^{a_2 t} (B\cos \omega_1 t - Bi \sin \omega_1 t) + e^{a_2 t} (C \cos \omega_2 t + Ci \sin \omega_2 t) + e^{a_2 t} (D \cos \omega_2 t - Di \sin \omega_2 t)$$

$$(30) \quad x_2 = (A'\cos \omega_1 t + A'i \sin \omega_1 t)e^{a_1 t} + e^{a_1 t} (B'\cos \omega_1 t - B'i \sin \omega_1 t) + e^{a_2 t} (C' \cos \omega_2 t + C'i \sin \omega_2 t) + e^{a_2 t} (D' \cos \omega_2 t - D'i \sin \omega_2 t)$$

Combining (29)and (30) using De Moive's Theorem

$$(31) \quad x_1 = e^{a_1 t} (C_1\cos \omega_1 t + C_2 \sin \omega_1 t) + e^{a_2 t} (C_3 \cos \omega_2 t + C_4 \sin \omega_2 t)$$

$$(32) \quad x_2 = e^{a_1 t}\,(C_1' \cos \omega_1 t + C_2' \sin \omega_1 t) + e^{a_2 t}\,(C_3' \cos \omega_2 t - C_4' \sin \omega_2 t)$$

where

$$C_1 = (A + B)$$
$$C_2 = (A - B)i$$
$$C_3 = (C + D)$$
$$C_4 = (C - D)i$$
$$C'_1 = (A' + B')$$
$$C'_2 = (A' - B')i$$
$$C'_3 = (C' + D')$$
$$C'_4 = (C' - D')i$$

BIBLIOGRAPHY

1. "A Study of Dynamic Forces in Aircraft Landing Gear Struts With Relation to the Optimum Angle of Suspension", H. Wood, A Thesis for Degree of Master of Science in Aeronautical Engineering, July, 1949.

2. "Results of Landing Tests of Various Airplanes", J. A. Hootman and A. R. Jones, NACA, Technical Note, No. 863.

3. "Loads On and Behavior of Landing Gears During the First Phase of the Landing Impact", Walter Boccius, Technical Report No. F-TR-1172-ND, Aug. 1948, Headquarters Air Materiel Command Wright-Patterson Air Force Base, Dayton, Ohio.

4. "Mathematical Methods in Engineering", Theodore V. Karman and Maurice A. Biot, McGraw-Hill Book Company, Inc., 1940, First Edition, Ninth Impression.

5. "Mechanical Vibrations", J. P. Den Hartog, McGraw-Hill Book Company, Inc., 1947, Third Edition, Second Impression.

6. "Advanced Dynamics", S. Timoshenko and D. H. Young, McGraw-Hill Book Company, Inc., 1948, First Edition.

7. "Higher Mathematic for Engineers and Physicists", Ivan S. Sokolnikoff, Ph.D., and Elizabeth S. Sokolnikoff, Ph.D., McGraw-Hill Book Company, Inc., 1941, Second Edition, Thirteenth Impression.

8. "Manual of Mathematics and Mechanics", Guy Roger Clements, Ph.D., and Levi Thomas Wilson, Ph.D., McGraw-Hill Book Company, Inc., 1937, First Edition, Sixth Impression.

9. "Aircraft Vibration and Flutter", C. R. Freberg and E. N. Kemler, John Wiley & Sons, Inc., Chapman & Hall, Limited, Copyright, 1944.

10. The Actual Loads on Airplane Landing Gear, by S. Shiskin, T.M. No. 821, NACA, 1937.

11. The Shock-Absorbing System of the Airplane Landing Gear, P. Callerio, T.M. No. 933, NACA, 1940.

Thesis 11475
T94 Turner
An investigation of dynamic stresses in a landing gear at a predetermined strut angle.